

# FEASIBILITY STUDY ON ELECTRIC POWER PRODUCTION BY THE HELIO - AERO - GRAVITY EFFECT

631.31  
GAN  
23

By

GANESH. B.  
JEEJA C. K.

## PROJECT REPORT

Submitted in partial fulfilment of the  
requirement for the degree of

**Bachelor of Technology**

in

**Agricultural Engineering**

Faculty of Agricultural Engineering & Technology  
Kerala Agricultural University

Department of Farm Power Machinery and Energy  
Kelappaji College of Agricultural Engineering and Technology

Tavanur - 679 573

Malappuram

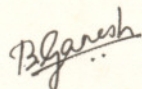
1993

# DECLARATION

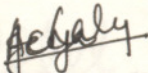
We hereby declare that this project report entitled "Feasibility Study on Electric Power Production by the Helio-Aero-Gravity Effect" is a bonafide record of project work done by us and this work has not previously formed the basis for the award to us of any degree, diploma, associateship, fellowship or other similar title, of any other University or Society.

Tavanur,

17 Nov., 1993.



GANESH B.



JEEJA C.K.

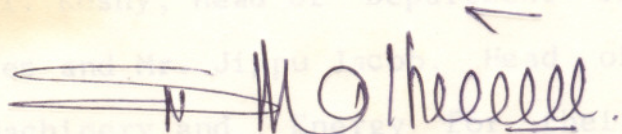


CERTIFICATE

Certified that this project report, entitled "Feasibility Study on Electric Power Production by the Helio-Aero -Gravity Effect" is a bonafide record of project work done jointly by Sri. Ganesh .B and Kumari Jeeja C.K. under my guidance and supervision and that it has not previously formed the basis for the award of any degree, diploma, fellowship, associateship or other similar title to them, of any other university or society.

Tavanur

17 Nov., 1993.



Sri. Sathyajith Mathew

Assistant professor

Department of Farm Power

Machinery & Energy

K.C.A.E.T.

## ACKNOWLEDGEMENT

We express our gratefulness to all the staff members and our friends, especially Satheesan, Sajl.K, Neeraj and Balakrishnan for the whole hearted help and cooperation extended towards us for the completion of this work. We avail this opportunity with great pleasure to express our profound and sincere sense of gratitude, indebtedness and affinity to our much respected guide Mr. Sathyajith Mathew, Assistant Professor, Department of Farm Power Machinery and Energy for his professional guidance, appraisal of the work at the hour of need, valuable advices, constructive criticism, critical suggestions and immense help through out the course of this project work.

We express our heartfelt thanks to Prof. K. John Thomas, Dean i/c, K C A E T, Tavanur, Prof. T.P.George, former Dean i/c, K.C.A.E.T., Dr. K.I. Koshy, Head of Department of Supportive and allied courses and Mr. Jippu Jacob, Head of Department of Farm Power Machinery and Energy for their constructive suggestions and constant encouragement throughout the progress of this work.

We extend our deep sense of indebtedness and gratitude to the workshop staff especially Sri. C. S. Krishnan, Sri. Aboobacker, Sri. Kannan, Sri. Vijayan and Sri. Shyam for the assistance and help rendered by them.



We express our gratefulness to all the staff members and our friends, especially Satheesan, Saji.K, Neeraj and Balakrishnan for the whole hearted help and cooperation extended towards us for the completion of this work.

The immense help given to us by Sri. Samkunju.M.G., Computer Programmer K.C.A.E.T. and Sri. Narayanan Nair, Engineer, V S S C, will always be gratefully remembered by us.

Our deep sense of respect and reverence are due to our parents whose support and constant encouragement throughout the course of the project enabled us to overcome many difficulties and complete the work. Last but not the least, we bow before God Almighty whose blessings have paved the way for this achievement.

*Dedicated to  
our Parents*

**GANESH. B.**

**JEEJA.C.K.**



# CONTENTS

Table No.	Title	Page No.
Chapter	Title	Page No.
2.	LIST OF TABLES	31
3.	LIST OF FIGURES	33
4.	LIST OF PLATES	35
	SYMBOLS AND ABBREVIATIONS USED	
I	INTRODUCTION	1
II	REVIEW OF LITERATURE	6
III	MATERIALS AND METHODS	34
IV	RESULTS AND DISCUSSION	50
V	SUMMARY	103
	REFERENCES	i-iv
	APPENDICES	
	ABSTRACT	

## LIST OF TABLES

17. Variation of Theoretical and Observed Power with Insolation and Time 72

Table No.	Title	Page No.
1.	Solar Central Receiver Power Plants	18
2.	Design Details of the Power Plant at Manzanares	31
3.	Key Data for Plants of Various Sizes	33
4.	Design Details of the Microscale Prototype SCPP at Tavanur	35
5.	Variation of Temperature with Time	52
6.	Variation of Temperature with Time	54
7.	Variation of Temperature with Time	56
8.	Variation of Temperature with Time	58
9.	Variation of Temperature with Time	60
10.	Variation of Temperature with Time	62
11.	Variation of Velocity and Insolation with Time	65
12.	Variation of Velocity and Insolation with Time	67
13.	Variation of Velocity and Insolation with Time	69
14.	Variation of Velocity and Insolation with Time	71
15.	Variation of Velocity and Insolation with Time	73
16.	Variation of Velocity and Insolation with Time	75

17.	Variation of Theoretical and Observed Power with Insolation and Time	78
18.	Variation of Theoretical and Observed Power with Insolation and Time	80
19.	Variation of Theoretical and Observed Power with Insolation and Time	82
20.	Variation of Theoretical and Observed Power with Insolation and Time	84
21.	Variation of Theoretical and Observed Power with Insolation and Time	84
22.	Variation of Theoretical and Observed Power with Insolation and Time	88
23.	Variation of Overall Efficiency with Time	91
24.	Variation of Overall Efficiency with Time	91
25.	Variation of Overall Efficiency with Time	94
26.	Variation of Overall Efficiency with Time	94
27.	Variation of Overall Efficiency with Time	97
28.	Variation of Overall Efficiency with Time	97



## LIST OF FIGURES

Fig.No.	Title	Page No.
1.	Stretched membrane concentrators	21
2.	A view of the Solar Bowl	23
3.	Experimental facility at Manzanares	29
4.	Elevation of the prototype plant at Tavanur	45
5.	Plan of the prototype plant at Tavanur	46
6.	Graph showing variation of temperature with time	53
7.	Graph showing variation of temperature with time	55
8.	Graph showing variation of temperature with time	57
9.	Graph showing variation of temperature with time	59
10.	Graph showing variation of temperature with time	61
11.	Graph showing variation of temperature with time	63
12.	Graph showing variation of velocity and insolation with time	66
13.	Graph showing variation of velocity and insolation with time	68
14.	Graph showing variation of velocity and insolation with time	70

15.	Graph showing variation of velocity and insolation with time	72
16.	Graph showing variation of velocity and insolation with time	74
17.	Graph showing variation of velocity and insolation with time	76
18.	Graph showing variation of theoretical and observed power with insolation and time.	79
19.	Graph showing variation of theoretical and observed power with insolation and time.	81
20.	Graph showing variation of theoretical and observed power with insolation and time.	83
21.	Graph showing variation of theoretical and observed power with insolation and time.	85
22.	Graph showing variation of theoretical and observed power with insolation and time.	87
23.	Graph showing variation of theoretical and observed power with insolation and time.	89
24.	Graph showing variation of overall efficiency with time	92
25.	Graph showing variation of overall efficiency with time	93
26.	Graph showing variation of overall efficiency with time	95
27.	Graph showing variation of overall efficiency with time	96
28.	Graph showing variation of overall efficiency with time	98
29.	Graph showing variation of overall efficiency with time	99

---

# LIST OF PLATES

SYMBOLS AND ABBREVIATIONS

Plate No.	Title	Between Pages
1.	Collector surface of the prototype SCPP at Tavanur.	49 & 50
2.	A view of the prototype SCPP at Tavanur.	49 & 50
3.	Suryamapi	
4.	Digital temperature indicator	49 & 50
5.	Vane anemometer	
6.	Electronic anemometer digital	49 & 50

Dept.

Department



# SYMBOLS AND ABBREVIATIONS

kg/s	-	
kW	-	kilo watt
Å <sup>h</sup>	-	angstrom hour
Al <sup>h/m<sup>2</sup></sup>	-	Aluminium hour per metre square
am	-	anti meridian display
cd	-	cadmium emitting diode
cm	-	centimetre(s)
CO <sub>2</sub>	-	Carbon di oxide semiconductor
Cr	-	Chromium
DC	-	Direct Current
Dept.	-	Department
DNES	-	Department of Non Conventional Energy Sources
MWe	-	mega watt energy.
ECU	-	European Currency Unit
mW/cm <sup>2</sup>	-	milli watt per centimetre square
eg.	-	example
et al.	-	and others
etc.	-	et cetera
fig.	-	figure
F P M E	-	Farm Power Machinery and Energy
GI	-	galvanised iron
i.e.	-	that is
J/kg °K	-	Joule per kilogram degree kelvin
K	-	kelvin
KCAET	-	Kelappaji College of Agricultural Engineering and Technology
kg/m <sup>3</sup>	-	kilogram per cubic metre

kg/s	-	kilogram per second
kW	-	kilo watt
kWh	-	kilo watt hour
kWh/m <sup>2</sup>	-	kilo watt hour per metre square
LCD	-	liquid crystal display
LED	-	light emitting diode
m	-	metre
MIS	-	metal insulator semiconductor
mm	-	millimetre
MS	-	mild steel
m/s	-	metre per second
MW	-	mega watt
MWe	-	mega watt energy
mW/cm <sup>2</sup>	-	milli watt per centimetre square
Ni	-	nickel
No.	-	number
Pa	-	Pascal
PP	-	pages
pm	-	post meridian
Proc.	-	Proceedings
PTI	-	Press Trust of India
PV	-	Photo Voltaic
PVC	-	Poly vinyl chloride
SCPP	-	Solar Chimney Power Plant

Si	-	silicon
Sl. No.	-	Serial number
SPPP	-	Solar Pond Power Plant
SPV	-	Solar Photo Voltaic
Te	-	Tellurium
USA	-	United States of America
USSR	-	Union of Soviet Socialist Republic
W	-	watt
$W/m^2$	-	watt per metre square
Wp	-	peak watt
WREN	-	World Renewable Energy Network
"	-	inch
$\mu m$	-	micro metre
&	-	and
\$	-	dollar
$\eta$	-	efficiency
/	-	per
%	-	per cent
$^{\circ}C$	-	degree celcius
$^{\circ}F$	-	degree Farenheit



## INTRODUCTION

The development of a country in the social, economic and industrial fronts is closely related to the quantum of input power available. Energy has been widely accepted as the key to human progress since the very dawn of civilisation. Future demands for energy are likely to go up on account of increasing population and due to gradual and steady improvement in living standards all over the world. This is particularly true with respect to the agricultural sector of our country because of its large rural population and the agro-economy base.

Today man relies on five main sources of energy. The fossil fuels- coal, oil and natural gas account for no less than 95% of the world wide consumption, the remainder coming from hydroelectric and nuclear power station (3% and 2% respectively) (Garg, 1982). The fossil fuels, which are unaffordably expensive for the third world, are fast depleting- by the present level of production and consumption, coal will last for 120 years, over 80% of the oil reserves would be consumed by AD 2020 and natural gas, would last only as long as the crude oil reserves exist. (Sukhatme, 1984). *It has been estimated that India's reserves of crude oil and*

natural gas may last for a few decades more. On the other hand, the reserves of coal will last a few centuries. (Sunavala, 1993).

Our environment have been constantly degraded and polluted by the emissions of conventional power plants. The coal burning plants have been subjected to continuous attack as the main source of acid rain and increasing levels of carbon di oxide in the atmosphere. Leafing through the data of last 10 years, it is evident that carbon di oxide emission in the atmosphere has doubled. This is mainly due to the excessive burning of coal, oil and gas which emit 67%, 54% and 37% carbon di oxide respectively per kg of fuel burnt (WREN Congress, 1992). Thermal power stations discharge large amount of waste heat causing thermal pollution in lakes and rivers and endangering plant and animal life. There are frequent shut downs of nuclear reactors due to accidents, causing the release of highly toxic radioactive materials into the environment. Some of the few remaining pollution free places on the earth have already become dumping grounds for the radioactive wastes from nuclear reactors. Large hydroelectric projects like the Sardar Sarovar displace large population from their villages resulting in immense hardship to them, causing huge financial burden on the government concerned to rehabilitate them.



Against this background, mankind has started turning his attention towards long-term permanent type alternative or renewable energy sources like solar energy, wind energy, wave energy, geothermal energy, etc. Renewable energy is always extracted from a flow of energy occurring in the environment. The energy is then returned to the environment, so no thermal pollution can occur on anything but a small scale.

About 70-80% of solar radiation -- both direct and diffuse -- is available in the form of short wavelength radiation. Solar energy is a very large, inexhaustible, non-polluting primary source of energy, available in plenty for longer duration in developing countries like India. Research and development activities are going on in different parts of the world to harness solar energy for different applications like electric power production, space heating, refrigeration, drying, cooking, desalination etc. Solar energy can now be stored by producing hydrogen, or by storing in other mechanical or electrical storage devices and can be concentrated in solar furnaces, to produce high temperatures. But, large scale production of solar electricity and its viable utilisation from an economic point of view have not yet succeeded.

Several technologies for converting solar energy into electricity have been developed. One of the most recent concepts proposed in this field is the production of electricity using the Helio-Aero-Gravity Effect or the Solar



Against this background, mankind has started turning his attention towards long-term permanent type alternative or renewable energy sources like solar energy, wind energy, wave energy, geothermal energy, etc. Renewable energy is always extracted from a flow of energy occurring in the environment. The energy is then returned to the environment, so no thermal pollution can occur on anything but a small scale.

Solar energy is a very large, inexhaustible, non-polluting primary source of energy, available in plenty for longer duration in developing countries like India. Research and development activities are going on in different parts of the world to harness solar energy for different applications like electric power production, space heating, refrigeration, drying, cooking, desalination etc. Solar energy can now be stored by producing hydrogen, or by storing in other mechanical or electrical storage devices and can be concentrated in solar furnaces, to produce high temperatures. But, large scale production of solar electricity and its viable utilisation from an economic point of view have not yet succeeded.

Several technologies for converting solar energy into electricity have been developed. One of the most recent concepts proposed in this field is the production of electricity using the Helio-Aero-Gravity Effect or the Solar

Chimney effect. This concept is still in its developmental stage and much work has to be done on the theoretical and practical aspects of this technology. A unique solar chimney power plant based on this concept is already in operation at Manzanares in Spain, producing an output of 50 KW of electricity.

About 70-80% of solar radiation -- both direct and diffuse falling on the land surface is converted into thermal energy. (Lodhi et al, 1991). Part of this heat is conducted into the lower layers of the soil, about one-third is released into the surrounding air and the rest is accounted for by losses in the form of reflection, convection, etc.

Solar chimney power plants essentially consists of blackened earth surface covered with transparent canopy, a centrally situated chimney and a wind turbine fixed inside the chimney. Three well known physical principles are combined in a solar chimney-- raising the air temperature using green house effect, producing draft by central chimney and energy conversion through wind turbine. Solar radiation falling over the transparent cover and reaching the collector is absorbed by the blackened ground surface and the air above it is heated. The warm air flows to the chimney and rises drawing fresh air into the canopy from the surrounding. Temperature difference between the warm air and fresh air is



trasferred to kinetic energy. This kinetic energy of moving air mass is imparted to the wind turbine causing it to rotate. A generator coupled to the turbine will convert this mechanical energy into electrical energy. The electrical power output from large solar chimney power plants can be fed to the power supply grid of the region or for other useful purposes.

A study was conducted in K.C.A.E.T Tavanur, to test the feasibility of the concept of electric power production by the solar chimney effect. A microscale prototype solar chimney was set up as part of this study. The major objectives of the study are;

- (i) to verify, establish and demonstrate the operationalisation of the concept
- (ii) to generate data correlating the physical parameters of the system with the power produced
- (iii) to determine the overall efficiency of solar chimney power plant in terms of energy conversion.



## REVIEW OF LITERATURE

The relevance of tapping solar radiations to meet our day-to-day energy needs, methods used for quantifying solar energy impinging on earth's surface and different technologies adopted for converting this undepletable abundant energy source to electricity are reviewed in this chapter giving special reference to solar chimney concept.

Solar energy can be defined to include all forms of energy renewably derived from solar radiation and used for human purposes. This definition includes not only "direct" solar energy derived from solar radiation that is intercepted by collectors deployed by humans (eg: solar cells, flat plate collectors), but also "indirect" solar energy intercepted by humans at sometime in a natural cycle after solar radiation strikes the earth (eg: hydro power, wind, ocean, thermal energy fuel from plants). Broadly construed, this definition also includes the chemical energy stored in food, fodder and non fuel plant products and even the energy in air used to dry materials, to ventilate by natural convection, or to heat space in warm climates.

The earth receives an annual energy from the sun amounting to  $1 \times 10^{18}$  kWh. This is equivalent to more than 5,00,000 billion barrels of oil or about 1000 times the energy

of the known reserves of oil or more than 20,000 times the present annual consumption of energy of the whole world ( Garg,1982 ). In the earth's elliptical orbit around the sun, outside the earth's atmosphere, the insolation on a surface perpendicular to the sun's rays varies from a minimum of  $1345 \text{ W/m}^2$  on July 4th (when the earth is farthest from the sun) to a maximum of  $1438 \text{ W/m}^2$  on January 2nd. The earth's atmosphere reflects and absorbs some of the solar radiation, so that total insolation at noon on a clear summer day is perhaps  $1300 \text{ W/m}^2$  at the top of Mount Everest and is about  $1000 \text{ W/m}^2$  on the desert at sea level.(Ford Foundation,1979).

In traversing the earth's atmosphere, solar energy is diluted by attenuation, local weather phenomena, and air pollution. Solar radiation - direct and diffuse is received only intermittently at any point on the earth, that, on the average, it is in the range of  $100\text{-}800 \text{ W/m}^2$ . The amount of solar energy incident on a horizontal surface ranges from 3.5 to  $7 \text{ kWh/m}^2/\text{day}$ . The most favourable sites for collecting and exploiting solar energy are confined to areas between latitudes  $35^\circ\text{N}$  and  $35^\circ\text{S}$  of the equator. These areas receive some 2000-3500 hrs of sunshine per year.(Garg, 1982).

## 2.1. Measurement of Solar Radiation

The measurement of solar radiation can either be



made by means of several types of instruments which will measure the heating effect of direct solar radiation and diffuse solar radiation or by the use of empirical equations.

### 2.1.1. Pyranometer

Pyranometer or Solarimeter is an instrument for measuring the solar irradiance from a solid angle of  $2\pi$  on a horizontal surface. The most common pyranometers are based on detection of difference between the temperature of black surface and white surface by thermopiles. These are primarily designed for use in a horizontal position and are fitted with a large white disc to shade the instrument body from solar radiation. The commonly used pyranometers at present are the Eppley Pyranometer, Kipp Pyranometer and the Yellott Solarimeter.

In India, a simple portable instrument called Suryamapi is used for quick measurement of the total solar radiation.

### 2.1.2. Pyrheliometer

A pyrheliometer is an instrument for measuring the intensity of direct solar radiation at normal incidence. Most pyrheliometers differ from pyranometers in that, mechanically they must follow the sun to measure only direct sunlight and



avoid the diffuse component. Direct solar radiation is measured by attaching the instrument to an electrically driven equatorial mount for tracking the sun. The pyrheliometers widely used are (i) the Angstrom Pyrheliometer, (ii) the Abbot Silver Disc Pyrheliometer and (iii) the Eppley Pyrheliometer.

### 2.1.3. Pyrradiometer

A pyrradiometer is an instrument for the measurement of both solar and terrestrial radiation, i.e., for net atmospheric radiation on a horizontal upward facing black surface at the ambient air temperature.

### 2.1.4. Pyrgeometer

Pyrgeometer is an instrument for the measurement of terrestrial radiation only.

### 2.1.5. Sunshine recorder

This instrument is used to measure the duration of bright sunshine in a day. Campbell - Stokes sunshine recorders are commonly used for this purpose.

### 2.1.6. Empirical Equations:

#### 2.1.6.1. Average Daily Global Radiation:

Angstrom (1924) and Page (1964) developed an

empirical relationship relating solar radiation and the amount of sunshine.

$$\frac{H_g}{H_o} = a + b \left( \frac{S}{S_{\max}} \right)$$

where

$H_g$  = monthly average of the daily global radiation on a horizontal surface at a location (  $\text{KJ/m}^2\text{-day}$  )

$H_o$  = monthly average of the daily extra-terrestrial radiation at the top of the atmosphere (  $\text{KJ/m}^2\text{-day}$  )

$S$  = monthly average of the sunshine hours per day at the location (h)

$S_{\max}$  = monthly average of the maximum possible sunshine hours per day at the location (h)

a and b = constants obtained by fitting data.

#### 2.1.6.2. Average Daily Diffuse Radiation.

Sukhatme, S.P. (1984), described an empirical equation developed by Liu and Jordan (1960) correlating the daily diffuse-to-global radiation ratio against the daily global-to-extra-terrestrial radiation ratio.

$$\frac{H_d}{H_g} = 1.390 - 4.027 \left( \frac{H_g}{H_o} \right) + 5.531 \left( \frac{H_g}{H_o} \right)^2 - 3.108 \left( \frac{H_g}{H_o} \right)^3$$



where  $H_d$  = monthly average of the daily diffuse radiation  
on a horizontal surface ( KJ/ m<sup>2</sup>- day)

Analysis of Indian data yielded the following linear equations.

$$\frac{H_d}{H_g} = 1.411 - 1.696 (H_g/H_o), \quad (\text{Modi et al, 1979})$$

$$\frac{H_d}{H_g} = 1.354 - 1.570 (H_g/H_o), \quad (\text{Gupta et al, 1979})$$

### 2.1.6.3. Hourly Global and Diffuse Radiation

ASHRAE (1972), devised a method for estimating the hourly variation of global and diffuse solar radiation falling on a horizontal surface.

$$I_g = I_b + I_d, \quad \text{where}$$

$I_g$  = hourly global radiation

$I_d$  = hourly diffuse radiation

$I_b$  = hourly beam radiation

$$= I_{bn} \cos \theta \quad \text{where}$$

$I_{bn}$  = beam radiation in the direction of the rays.

$\theta$  = angle of incidence on a horizontal surface.



## 2.2. SOLAR ELECTRIC CONVERSION TECHNOLOGIES

### 2.2.1. Direct Electricity Generation using Photo-voltaic Solar Cells

Photovoltaic cells consists of thin wafers of silicon which are chemically treated to divide them into two layers which possess different electric potential. When the cell receives sunlight an electric charge is generated which by the difference in potential between the two layers is separated into positive and negative. An external electric circuit then collects the electricity thus generated. This simplicity of operation, in principle, makes photovoltaic cells an ideal solar energy technology.

It was reported (WREN Congress,1992 ) that thin film efficiency of a Si is very stable at system efficiency of 10.5%, while Cd Te cells achieved 17.5% in the laboratory. Further, crystalline silicon has achieved an efficiency of 15.5% while poly-crystalline silicon has reached 13.5%. PV systems of about 250MW capacity are installed around the world. To date,the high cost of PV systems has made them unattractive where mains connection is easily achievable.The present cost of an installed photovoltaic system is about \$5/Wp and the goal is to reduce this figure to \$0.06 by the

year 2005, when about 10,000MW will be installed in various parts of the world.

Shousha, A.H.M. (1988) reported a study conducted on the performance characteristics of thin film metal/insulator/semiconductor solar cells in terms of their physical parameters. It was shown that conversion efficiencies acceptable for terrestrial application could be achieved by proper choice of cell parameters. The results presented indicated that for silicon MIS cells with black-surface field, conversion efficiencies of 10-15% could be obtained using 5-25  $\mu$ m thick cells with minority carrier diffusion lengths of 10-100  $\mu$ m and interfacial layer 15  $\text{\AA}$  thick.

Wolde-Ghiorgis (1989) detailed the performance of a 10.5 KW photovoltaic system installation at a village in Ethiopia. The pilot plant had been supplying electrical energy to 390 house holds for night time lighting. The system basically comprised of solar collector arrays in conjunction with storage batteries, control subsystems, regulators and inverter circuits. The study showed that only about 6% of the available solar energy was fed to storage batteries and the final energy utilization amounted to about 3.9% of the incident solar radiation.

Shaefer et al (1992) compared photovoltaic power



generation and other renewable generation forms with conventional generation forms in terms of some environmental characteristics. A comparative analysis of the surface and material requirements of different power stations was given. The result of a detailed investigation about the accumulated energy consumption in the manufacturing and the construction of photovoltaic power plants and corresponding data about the  $CO_2$  emissions caused by photovoltaic power generation were presented.

Anonymous (1993) reported in The Times of India the construction of Asia's largest solar photovoltaic power plants rated at 100 kW capacity at Kalyanpur village in Uttar Pradesh. This power plant in addition to providing electricity to the entire village, supplied electricity during the day time to about 25 high efficiency solar photovoltaic pumping stations which would replace the current diesel driven pumping sets.

### 2.2.2. Solar Thermal Power Generation.

Although there have been a number of reported attempts over the last 100 years, to produce mechanical power from solar energy by using steam engines, the production of electricity by attaching a generator to the steam engine came only after the 1973 energy crisis.

Strub, A.S. of the commission of the European Communities, Brussels, reported the classification of solar thermal power generation systems in to three -

a) Large (1-100 MW) plants using many hundreds of heliostats directed onto a central receiver (tower) producing steam - has overall efficiency of 10 % and actual cost is around 25,000 ECU per installed KW. (1 ECU = 1.2 U.S.\$ )

b) Medium power systems using distributed mirror receiver fields (solar farms)- overall efficiency = 10 % and cost = 20 000 ECU/ KW.

c) Small sized systems based on high performance flat plate collectors, evaporating a low boiling point fluid which drives a special turbine or piston engine. Such systems have a very low overall efficiency of 1%, need too much maintenance and too costly at 50 000 to 1 00 000 ECU/KW.

#### 2.2.2.1. Central Receiver Power Plant.

In this system an array of heliostats reflect solar radiation onto a receiver mounted on top of a central tower, where it is removed as heat by means of a heat transport fluid and converted into electrical energy in a turbine generator.



Torrallbo et al (1983) reported the construction of a 1.2 MW Spanish power tower solar system named Project CESA 1 in Almeria, Spain. The technical concept selected consisted of a central receiver power plant with a water-steam cooled receiver, molten salt thermal storage and water-steam Rankine Cycle. The collector system included three hundred heliostats distributed in sixteen rows. The receiver system consisted of a cavity-type water-steam cooled reservoir, and 80 m concrete tower and the auxiliary piping system. The turbo generator was the main component of the power conversion system. The storage system contained two tanks- hot and cold- and two molten salt loops with conventional shell and tube type heat exchangers and vertical centrifugal pumps.

Radosevich et al (1988) reported in detail the operation of the 10 MWe Solar One Central Receiver Pilot PLant near Batstow, California. 1818 computer controlled heliostats reflected the solar energy on to the receiver consisting of tubes welded onto twenty four panels mounted on a central tower. Water was used as the heat transfer medium. Solar One generated a peak output of 11.7 MWe. The plant achieved a maximum monthly system efficiency of about 8.7 percent.

Anonymous (1993) reported in 'Global Technoscan', the proposed construction of a Solar Two Plant, at the same site as Solar One, using its 1818 heliostats and 300 foot

tower. This plant will use a nitrate salt that melts at 450o F, as the heat transfer medium.

Sukhatme, S.P (1992) discussed the technologies and systems developed for the generation of electricity from solar thermal energy. The author reported that seven central receiver power plants had been built in the eighties. All these plants were pilot plants and had outputs ranging from 0.5 to 10 MWe. (Table 1).

Although all the central receiver plants had been operated succesfully, the data in table 1 indicated that they were very costly.



Table 1. Solar Central Receiver Power Plants. (Sukhatme, 1992)

Plant name	Location	Output (MWe)	Receiver type	Receiver fluid	Start of operation	Construction cost per KW in U.S.\$
SSPS	Spain	0.5	Cavity	Sodium	1981	41 000
EURELIOS	Italy	1.0	Cavity	Steam	1981	---
CESA 1	Spain	1.0	Cavity	Steam	1981	11 000
SUNSHINE	Japan	1.0	Cavity	Steam	1981	33 000
THEMIS	France	2.0	Cavity	Molten salt	1983	15 000
CES 5	USSR	5.0	External	Steam	1985	----
SOLAR ONE	USA	10.0	External	Steam	1982	14 000

Zvirin et al (1993) reported the installation of an experimental 250 KW Ormat gas turbine at the Weizmann Institute Solar Tower in Israel. A ceramic receiver was used to heat pressurized air to about 1000o C. The hot air was expanded through a gas turbine driving the generator.

#### 2.2.2.2. Distributed Receiver System

Large number of collectors ( flat plate, parabolic troughs or parabolic dishes ) with its own absorber, is distributed over a large area. Each collector is connected to the forward flow tubes and the return flow tubes of the central thermal power machine. The transfer of energy from the absorber is achieved by a heat transfer fluid.

Boy-Marcotte et al (1982) described the construction of a 100 KW solar thermal- electric experimental plant in Corsica, France. The plant consisted of a field of 71 flat reflecting concentrators producing heat at 250oC, a stratification thermal energy storage of about 1250 kWh, two power conversion units of 45 kWe each, with a supersonic turbine and two cooling towers of 200 kW each.

Schlaich et al. (1992) reported the construction of three systems of stretched membrane concentrators with stirling engines in Almeria, Spain. The system consisted of a parabolically curved concentrator. It tracks the sun and



concentrates the radiation to a receiver positioned in its focal point where a gas is heated. The radiation energy thus converted into heat is conducted to a stirling engine. The thermo dynamic power engine transforms the heat into mechanical energy and, with a generator directly attached, into electrical energy. The diameter of the concentrator was 7.5m and the electrical output 9kW. The authors also reported the installation and working of two 50kW concentrators in Riyadh, with a diameter of 17m each, as well as a 7.5 kW / 7.5 m prototypal installation in Stuttgart. A view of the concentrators in Almeria is shown in fig. 1.

Sukhatme, S.P. (1992) reported the development of line focussing parabolic collector and paraboloidal dish collector technologies. The first commercial line focussing parabolic collector plant having a capacity of 14 MW was commissioned in 1984. Since then 6 plants of 30 MW capacity each followed by two plants of 80 MW each had been installed. All these plants were located in California. The author also reported that the Indian experience with the line focussing parabolic collector technology was restricted to a small 50 kW capacity experimental plant installed at the Solar Energy Centre of the DNES. A 30 kW power station near Hyderabad utilizing four paraboloidal dish collector modules were reported by the author as the only one of its kind in the



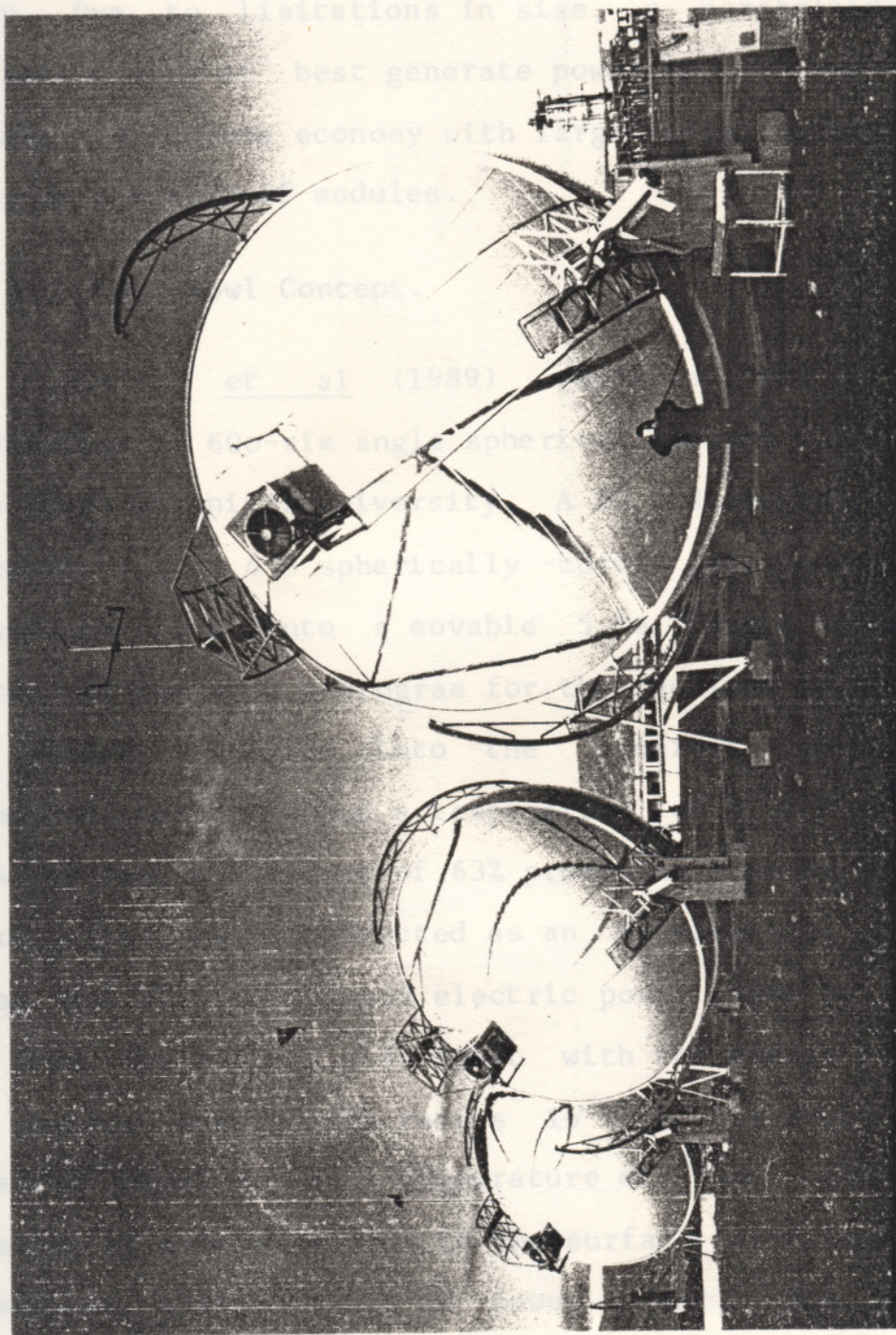


Fig.1 Stretched membrane concentrators



country. Due to limitations in size, a paraboloidal dish collector could at best generate power in kW and it was difficult to achieve economy with large scale generation by linking up a number of modules.

#### 2.2.2.3. Solar Bowl Concept.

Lodhi et al (1989) reported the successful demonstration of 60°-rim angle spherical bowl on a small scale at the Texas Technical University. A 20 m diameter spherical bowl consisting of 438 spherically -curved glass mirror panels focussed the sun onto a movable 5.5m long receiver. A computer is fed with a program for the receiver to track the sun. Water supplied into the receiver turned into superheated steam to about a temperature of 810° K working at a measured peak efficiency of 63% providing a power output of 250 kW<sub>th</sub>. This was constructed as an experimental plant to develop a 5 MW solar hybrid electric power plant to serve a small town. The authors also dealt with the design parameters of a shallow bowl of rim radius 16 m and rim angle of 40°. The steam developed at a temperature of 750°F, assuming an insolation of 850W/m<sup>2</sup> normal to the surface for 6 hours, could be used to operate a 150 kW power plant. The schematic representation of the concept is shown in fig.2.

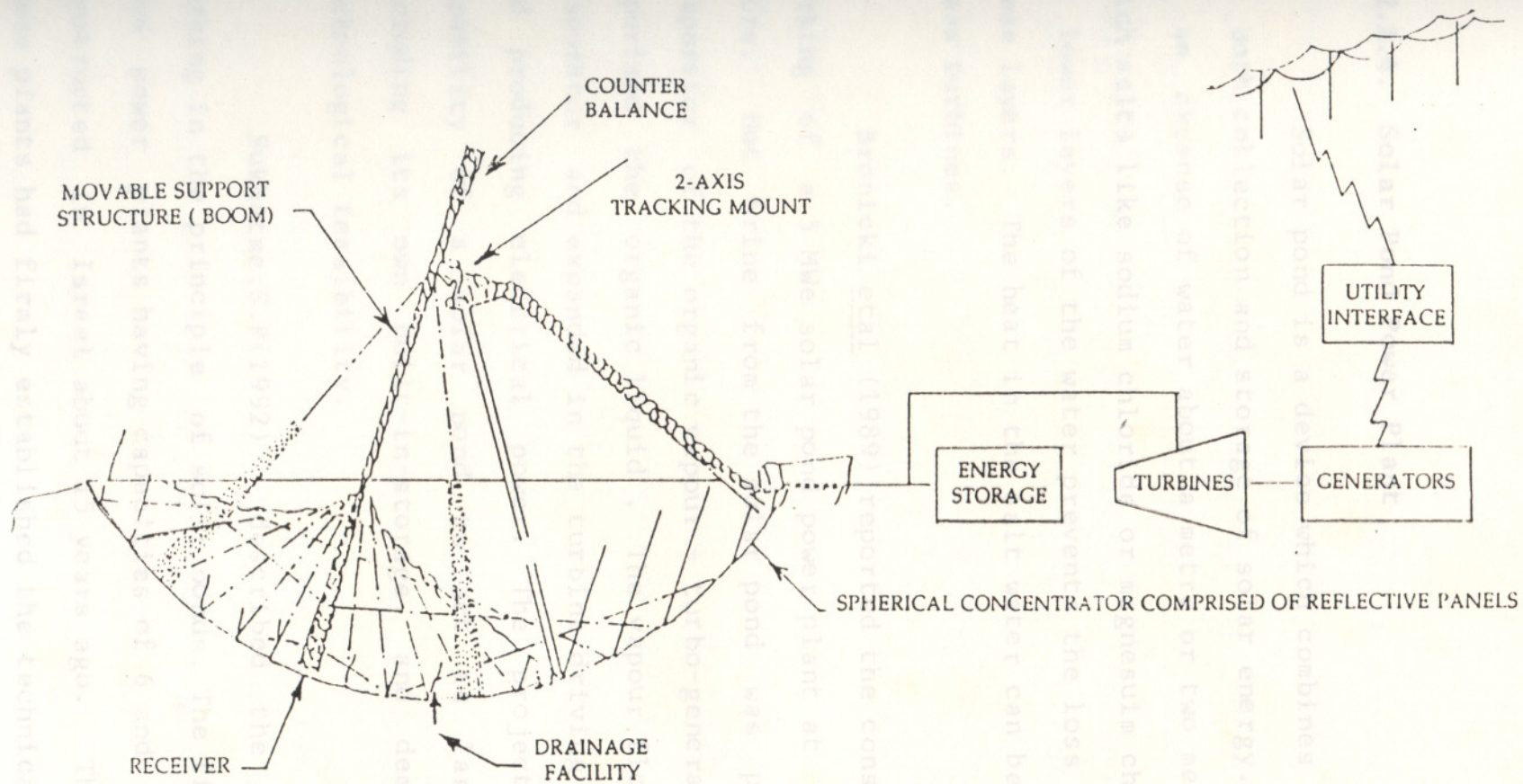


Fig. 2 A View of the Solar Bowl



#### 2.2.2.4. Solar Pond Power Plant

Solar pond is a device which combines the functions of both collection and storage of solar energy. It consists of an expanse of water about a metre or two metres deep in which salts like sodium chloride or magnesium chloride added to lower layers of the water prevents the loss of heat from these layers. The heat in the salt water can be used to drive steam turbines.

Bronicki etal (1989) reported the construction and working of a 5 MWe solar pond power plant at the Dead Sea shore. Hot brine from the solar pond was pumped to the evaporator of the organic vapour - turbo-generator where it vapourised the organic liquid. The vapour flowed from the evaporator and expanded in the turbine driving the generator and producing electrical power. The project showed the capability of a solar pond to act as large collector, including its own built-in-storage, and demonstrated the technological feasibility.

Sukhatme, S.P (1992) described the power plants working in the principle of solar ponds. The first two solar pond power plants having capacities of 6 and 150 KWe were constructed in Israel about 15 years ago. The working of these plants had firmly established the technical viability of

serious adverse environmental consequences and would have to be collected on large areas away from population centres. The loss in collection, conversion, transmission, and distribution on earth would be large. The cost would also be immense.

#### 2.2.5. STATUS OF RESEARCH ON SOLAR CHIMNEYS

This concept is relatively young, introduced in the beginning of 80's. Researches were conducted and is continuing, mainly in the U.S., Germany and Spain, regarding the feasibility and installation of large power plants. A brief review of the limited work done in this field and the features of a 50 kW solar chimney power plant at Manzanares, Spain is dealt with.

Kulunk (1985) undertook a study for electric power generation on a prototype solar chimney of 9m<sup>2</sup> area and chimney height of 2m in Izmit, Turkey. A generator rotor of 8 wings made up of aluminium plate of 0.005m thick was used. Generator started to work at air velocity of 7m/s and the power produced was calculated as 0.14W via current and potential difference across the generator. On a particular day, the pressure difference measurements along 2m chimney predicted a maximum of 200Pa and a temperature difference of 40C was detected in the air flow between entrance and exit of the chimney.



Scesa (1985) conceptualised that large hyperbolic cooling towers of abandoned nuclear power plants could serve the function of solar chimneys, with transparent cover several feet above the ground surrounding the tower base as solar collector and a turbine inside the tower. A theoretical analysis for estimating the power available as a function of tower configuration and solar collector area was conducted. A typical hyperbolic cooling tower configuration along with five modified internal configurations were examined. The results showed that the power available increased as the collector diameter increased and was very sensitive to the internal configuration. The cylinder cone shape with the turbine located at the exit plane provided the highest output. The annual energy output for the cylindrical conical configuration and a collector diameter of 1600m was estimated. The author found that efficiency will be equal to  $1/6$  if it was assumed that 40% of the solar energy available is gained by the air flowing under the collector area with the remaining 60% gained by the ground. This value along with the air flow attained during night with an assumed efficiency of  $1/10$ , generated an energy output of 64 million KWh per year. The author also suggested after obtaining preliminary data by extending the cylindrical configuration by 30.5m that the available power could be increased by about 10% .



Lodhi et al (1991) carried out a systematic theoretical study to investigate the scientific and technical merits of the solar chimney system for large scale power production, dealing with the heat transfer processes in the system in a quantitative manner. The authors are of the opinion that economic and efficient power production from the helio-aero-gravity concept can be achieved in isolated deserts where solar radiation is abundant. Model calculations for convective heat transfer were developed with some reasonable assumptions, taking the helio-aero effect and chimney effect separately. Formula for calculating the rotor power including both helio - aero and chimney effect was developed. Increasing the chimney height and / or its radius increased the efficiency of the plant. The efficiency was reduced when the area of the collector and the canopy gap at the periphery were increased. The authors concluded that the power production maximised at large values of surface temperature and this required a selective surface with large co-efficient of absorption.

Schlaich et al (1992) with assistance from the German Federal Ministry for Research and Technology, designed and developed an experimental solar chimney power plant at Manzanares in Spain. (Fig.3).The aim of the project was to establish the energy conversion principle and to evaluate the



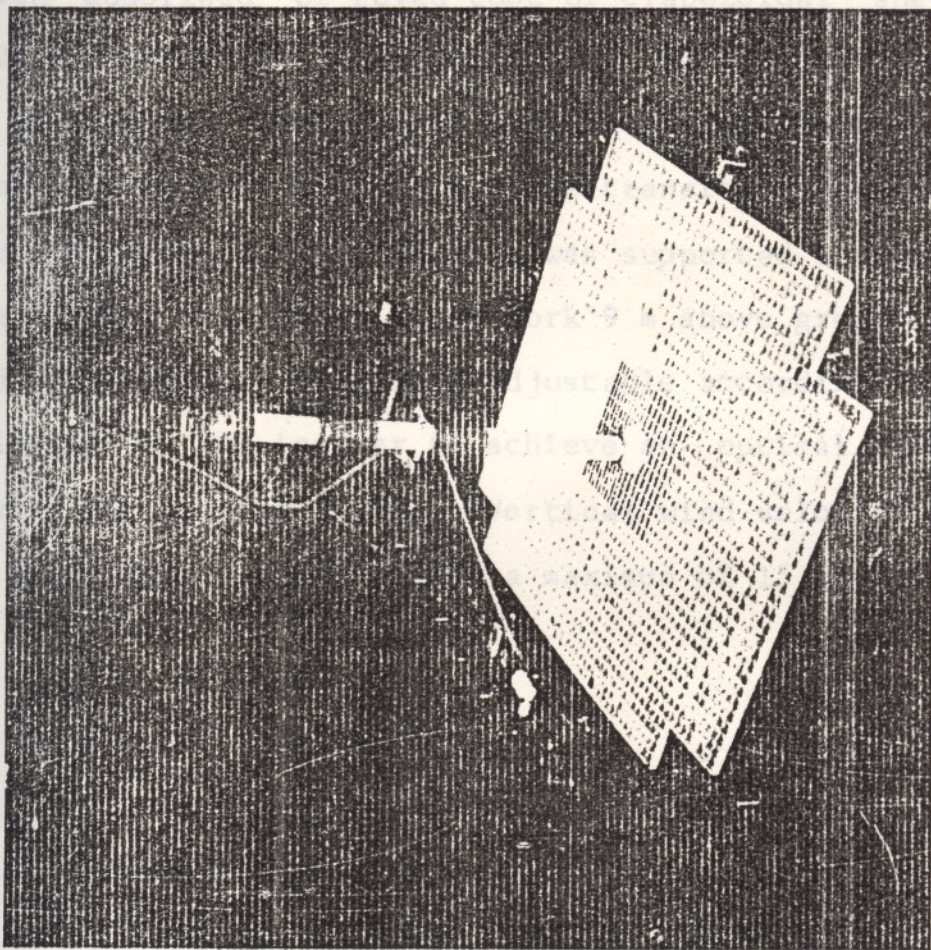


**Fig. 3** Aerial photograph of the experimental facility at Manzanares, Spain. (Height of chimney, 119 m; chimney radius, 5 m; mean radius of collector, 119 m; rotor diameter, 10 m; nominal speed, 100 rpm.)

Table 2. Design details of the power plant at Manazamara technical and economic potential of the system. The design details of the plant are reproduced in table 2. The chimney which comprised of guyed tube of trapezoidal sheets, gauge 1.25 mm, stood on a supporting ring 10 m above ground level. A prestressed membrane of plastic-coated fabric, with good flow characteristics, formed the transition between the roof and the chimney. The turbine was supported independently of the chimney on a steel frame work 9 m above ground level. It had four blades which were adjustable according to the face velocity of air in order to achieve an optimal pressure drop across the turbine blades. Vertical wind velocity was 2.5 m/s on start up and could attain a maximum of 15 m/s.



Table 2. Design details of the power plant at Manazanares  
(Schlaich,1992)

Height of chimney	194.60 m
Radius of chimney	5.08 m
Mean radius of collector	122.00 m
Height of collector roof	1.85 m
Number of rotor blades	4
Diameter of the rotor	10.00 m
Speed of the rotor	100 rpm
Solar radiation	1 000 W/m <sup>2</sup>
Heating in collector, $\Delta T$	20 °C
Efficiency of collector	32%
Efficiency of turbine	60%
Updraught - under load	9 m/s
Updraught on release	15 m/s
Roof covered with plastic	40000 m <sup>2</sup>
Roof covered with glass	6000 m <sup>2</sup>
Design power output	50 kW

A whole series of experiments were performed on the plant, the results of which showed the dependable and highly reliable operation of the components and the plant as a whole. A thermo dynamic simulation program that describes the individual components, their performance and their dynamic interaction was developed. Thermodynamic behaviour of large scale plants under given meteorological conditions could be calculated in advance using this program.

Extrapolation of the results to larger plants produced the results summarised in table 3. The authors suggested substantial increase in the plant efficiency when partial or total double glazing was used for the collector and when IR coated glass was used. The specific electricity generating costs were calculated and found to be comparable with those of conventional power plants. The authors estimated that solar chimney power plants rated at around 100 MW could generate electricity at approximately \$ 0.10/ KWh.



Table 3. Key Data for Plants of Various Sizes.

(Schlaich, 1992)

Parameters	Power Rating and Location			
	50 kw Manzanares	4 mw Manzanares	5 mw Barstow	200 mw Barstow
Geographical latitude (degrees)	39.05	39.05	34.05	34.05
Global radiation ( $W/m^2$ )	200.7	200.7	292.3	292.3
Wind velocity (m/s)	4.0	4.0	3.5	3.5
Annual total global radiation ( $kWhr/m^2$ )	1758.1	1758.1	2560.8	2560.8
Chimney height (m)	194.6	445	445	1000
Chimney radius (m)	5.08	28	28	92
Collector radius (m)	119	555	555	2500
Type of turbine	Propeller type wind turbine			
No. of turbines	1	27	31	230
Rotor diameter (m)	10	10	10	25
No. of blades	4	4	4	4
Annual energy output (MWhr)	42	7170	11600	582140
Overall solar plant efficiency (%)	0.053	0.43	0.47	1.10
Mass flow rate (tons/sec)	0.630	24.00	26.80	426.50
Total operating time (hr)	4860	8740	8740	8656
Full-load operating hours of system (hr)	1158	1811	2523	2526

## MATERIALS AND METHODS

Table. 4 Design details of the microscale prototype solar chimney plant at Tavanur

A general description of the microscale prototype solar chimney plant, the materials used for the construction of the plant, the construction stages and the test procedures are presented in this chapter.

### 3.1. General description of the Plant

The microscale prototype solar chimney plant consisted of a solar chimney placed at the centre of a transparent canopy spread at a height above a painted black surface. The height of the canopy was maximum at the centre, where it was attached to the chimney. At the periphery of the collector, the canopy could be kept raised at three separate heights from the ground surface. The design details of the solar chimney plant is given in table 4.



Table. 4 Design details of the microscale prototype solar chimney plant at Tavanur

---

Size of collector	: 6m x 6m
Height of chimney	: 6 m
Diameter of chimney	: 25 cm
Canopy gap at periphery	: 17, 32, 47 cm
Canopy gap at centre	: 80 cm

---

The selection of site for installing the plant and the materials required for the study were decided keeping in view the main objective of testing the feasibility of the concept.

### 3.1.1. Site selected

A large open area adjacent to the F P M E department and the college library was chosen for installing the solar chimney plant. Two factors favoured the selection of the site.

1. Large open area receiving good insolation
2. Minimum obstructions near the site

A 6m x 6m plot inside this area was selected as the exact location of the solar chimney plant.

### 3.1.2. Collector surface

Readily available materials like sand, stone and cement were used to prepare a cemented collector surface about 2 to 3 cm thick on the ground. Cement surface was chosen to get a higher surface temperature than can be produced by natural ground. The collector surface was given three coatings of ordinary black paint to increase the absorptivity of the surface to solar radiations. (Plate 1).



### 3.1.3. Canopy

Strips of transparent clear plastic sheet of medium strength and durability was hot pressed into a single square cross section of size 7m x 7m. This sheet was placed at varying height above the collector surface, supported on GI wires, with the maximum height at the centre and minimum height at the periphery. Eight angle iron pieces ( 1 & 1/4" and 1/4" ) of length 1m each formed the supports at the four corners of the plot and at the mid points of the sides. About 45 cm length of these angle irons were buried in concrete in the ground inclined at a small angle to the vertical towards the outside. Three 5/8" holes were drilled on the protruding portion at heights of 17 cm, 32 cm and 47 cm from the ground for guiding and fixing the bolts of the tightening device. 14 gauge GI wires connecting the bolts and the hooks on the middle support for the chimney, formed the main support for the transparent sheet. GI wires were also connected laterally at 0.5 m, 1.5 m and 2 m from the centre to prevent the transparent sheet from sagging too much.

### 3.1.4. Solar Chimney

A PVC pipe of height 6 m and inside diameter 25 cm was used as the chimney. Three MS rods of 18 cm diameter and 120 cm length were used to fabricate the support for the solar

chimney. Two MS flats of one inch and one and a half inch width respectively were used one above the other to form the base support of the solar chimney.

The MS rods were welded on to the bottom flat piece from the side at equal spacing so that the top of the MS rods coincided with the top of the bottom MS flat. Eight hooks each having inside diameter of one inch, made out of 1/8 MS rods were welded at equal spacing onto the side bottom of the bottom MS flat.

The radial GI wires connected between the bolts and hooks had to be tightened to a very high degree to prevent the sagging of the transparent sheet. The tightening device on each of the angle irons consisted of a grooved bolt and nut, with a key to guide the bolt without turning, and a collar for fixing the device on to the angle iron.

The chimney was guyed at about  $2/3_{rd}$  height from the bottom along three directions at 45° to the vertical using 14 gauge GI wire.

### 3.2. Installation procedure

The 6 m x 6 m square area was fixed on comparatively lesser rocky terrain for the purpose of easy installation and levelling of the ground. The whole area was covered with 2-3



cm thick cement plaster and a thin coating of grout with minimum degree of roughness was also applied. The setting of cement surface was followed in the next stage by the application of black paint to the surface. Black colour has a high degree of absorptivity for solar radiations as well as high emissivity for thermal radiations. Selective black coatings like cobalt black and black chrome are recommended but due to the highly expensive nature of these coatings, ordinary black paint was applied in three coatings on the surface.

The support to the transparent plastic sheet was then laid by connecting the GI wires between the central chimney support and the bolts placed in the middle hole of the angle iron and also crosswise between the radial wires. The wires were tightened by turning the nuts. The transparent sheet was then laid over the wire support. Keeping one half of the sheet rolled upto the centre, the PVC pipe, on which the stay wires had already been clamped, was guided through the hole in the sheet to its seat and erected vertically by tightening the stay wires to outside hooks clamped to the ground. The sheet was fixed at the centre to the pipe using cellotapes and tied around to prevent detachment from the pipe. At the periphery, the excess width of the sheet was

folded and fixed using cellotapes to allow gap for the entry of air into the plant. (Plate 2).

### 3.3. Instrumentation

#### 3.3.1. Suryamapi

The intensity of solar radiation is read from the instrument named 'Suryamapi'. It is a hand held portable solar intensity meter, used for the measurement of total global solar radiation. The meter is calibrated against AMI radiation for both  $\text{mW/cm}^2$  and langley/hr. (Plate 3).

Suryamapi uses a specially fabricated silicon cell which is connected through a suitable circuit to a current meter. The sensing solar cell is mounted at the top of the meter. The response of the sensing element is linear over a wide range of intensities. Suryamapi is kept perpendicular to the incident radiation and the corresponding deflection on the scale indicates the intensity. The intensity is measured in  $\text{mW/cm}^2$  and is recorded in the table as  $\text{W/m}^2$ . The specification of the instrument is given in Appendix I

#### 3.3.2. Thermometer

Temperature measurements are taken using two types of thermometers.



### 3.3.2.1. Mercury thermometer.

This thermometer gives the direct readings of temperatures in degree celcius corresponding to the level of mercury column. Specification of the instrument is given in Appendix I.

### 3.3.2.2. Digital thermometer

The digital thermometer consists of a LCD display temperature indicator and thermocouple sensors for use at various places. Thermocouples are widely used for solar collector testing. A thermocouple is formed by joining together two wires made of dissimilar metals. Suitable pairs of thermocouple materials are Copper/Constantin, Iron/Constantin and Chromel/Alumel. The temperature indicator is fitted with standard K probe socket and can match any standard type K (NiCr-NiAl) sensor. The circuit used in the instrumentation provides high accuracy and wide measurement range. Power is supplied from a DC 9V battery. Sensors for taking temperature measurements from flat surface as well as from air are provided. The specification of the instrument is given in Appendix I.(Plate 4).

### 3.3.3. Anemometer

Anemometer is an instrument to measure wind

velocity. Measurements are taken using two types of anemometers.

### 3.3.3.1. Vane Anemometer

A vane anemometer consists of a number of vanes supported on short radial arms and mounted on a spindle. It is a directional transducer which measures the air speed in the direction of spindle axis. A dial attached to the spindle gives the cumulative readings of the distance measurement for a particular time period. Mechanical freeze facility to stop the rotation of the needle is also provided. The specification of the instrument is given in Appendix I. (Plate 5).

### 3.3.3.2. Electronic anemometer digital

It consists of a vane type wind sensor connected to a suitcase-mounted instrumentation with a LED display (Plate 6). The instrument can be operated on mains or batteries. Provision for taking the output in a recorded form is also given. The instrument performs accurately to wind velocities of upto 30 m/s. The specification of the instrument is given Appendix I.

## 3.4. Testing methodology

The test was performed in the prototype plant during



the days when it was felt that the insolation was somewhat conducive to give reliable data. The mode of taking measurements from the plant during the testing phase was concentrated towards obtaining the maximum values of output power and mass flow rate of air. This method was adopted for some days because the sky was overcast most of the time and good sunshine was received only for 1-2 hours daily. The plant was also tested continuously when the solar radiation was received without break.

The datas which will help in understanding the characteristics of air inside the canopy enclosure and the chimney and also outside the plant were obtained. These datas included solar insolation, ambient temperature of air, temperature of air at the bottom of the chimney, velocity of air inside the chimney and the temperature of the collector surface. Mercury thermometer was used for measuring the ambient air temperature. All other temperature measurements were made using the digital temperature indicator with thermocouple temperature sensing units. The velocity of air inside the chimney was sensed using the electronic anemometer. The outside wind velocity was measured using the vane type anemometer. A suryamapi was used to determine the solar insolation.

It was clear after installing the plant, that the canopy gap at the periphery will have to be kept limited to prevent the effect of side winds. Keeping this in view this height was kept at 17 cm from the ground level, which was the lowest adjustment possible in the plant set up. The elevation and plan of the plant set up are shown in fig. 4 and fig. 5.

The datas obtained from the tests conducted were utilised to determine the various air related characteristics, power output and efficiency of the prototype solar chimney plant.

### 3.4.1. Mass flow rate of air

The mass flow rate of air entered at the periphery which continues to travel through the space under the canopy until it reaches the chimney and finally exits from the top of the chimney is given by the continuity equation.

$$\dot{m} = A_p \cdot u \cdot \rho_a = A_c \cdot v \cdot \rho_m$$

where  $\dot{m}$  = mass flow rate of air (Kg/s)

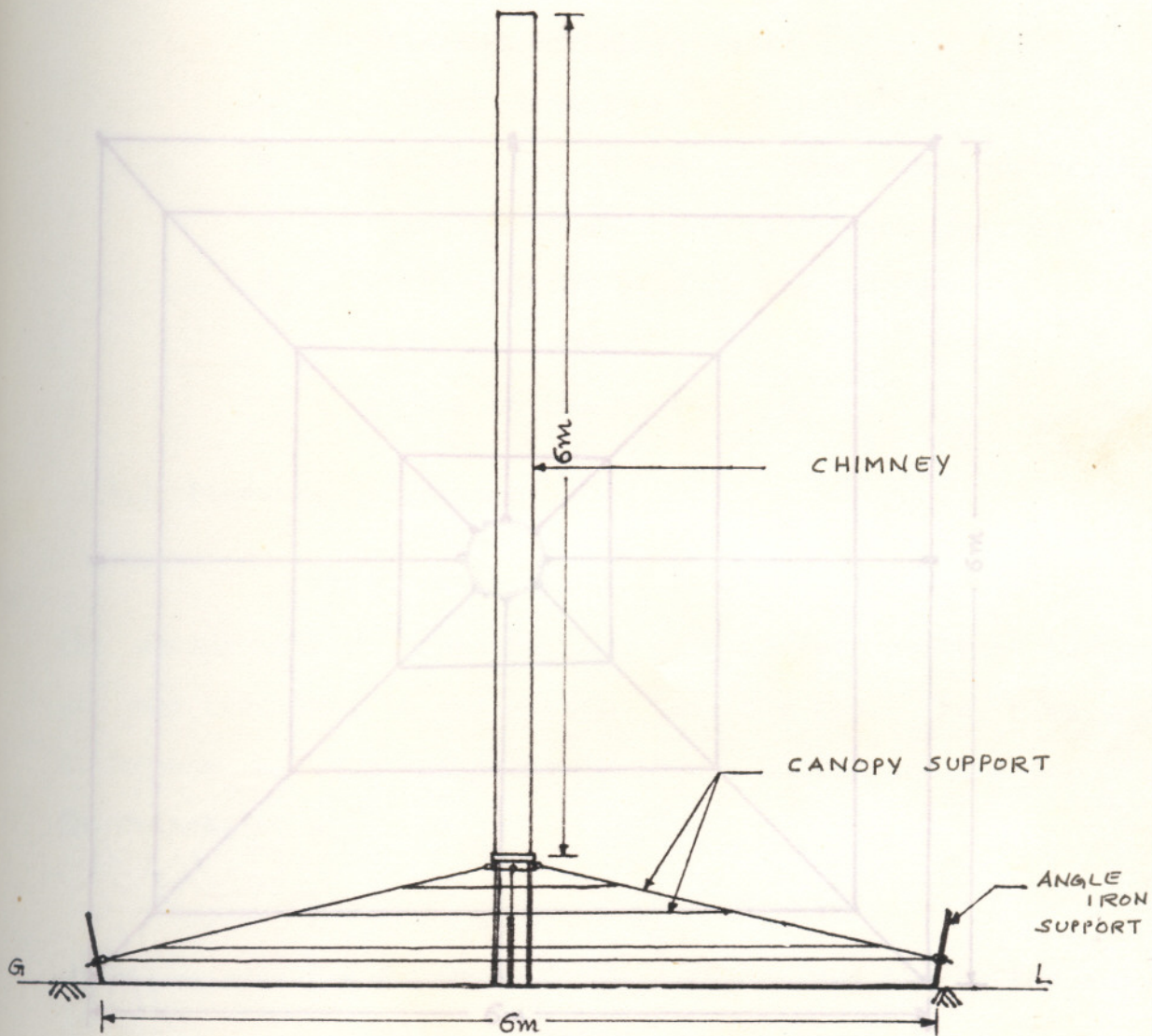
$A_p$  = Area at the periphery of the canopy through which air enters the plant

$$= 4 \cdot L \cdot H_p$$

where  $L$  = Length of the side of the collector (m)

$H_p$  = Height of the canopy at the periphery (m)

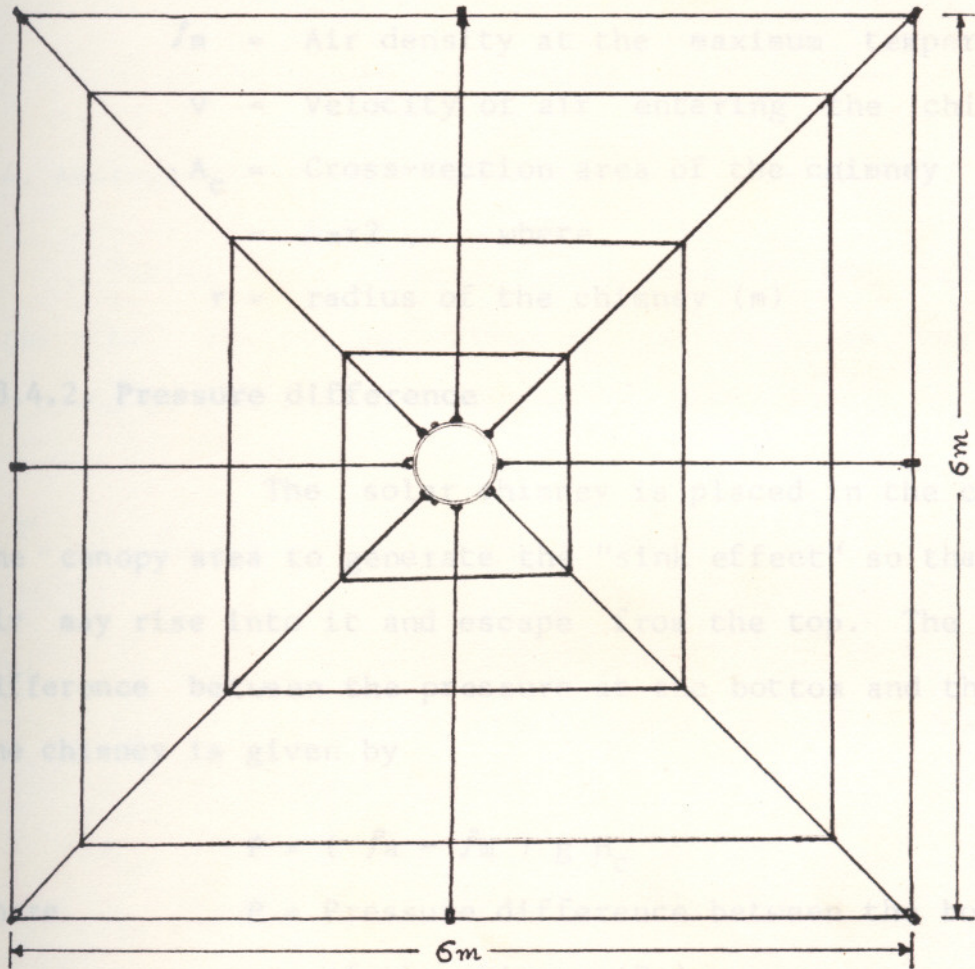




Scale: 1:50  
 Scale: 1:50

Fig.5 Plan of the prototype plant at Tavanur

Fig.4 Elevation of the prototype plant at Tavanur



Scale: 1:50

Fig.5 Plan of the prototype plant at Tavanur



$u$  = Incoming velocity of the air at the collector periphery (m/s).

$f_a$  = Ambient density of air ( $\text{Kg/m}^3$ )

$f_m$  = Air density at the maximum temperature ( $\text{Kg/m}^3$ )

$v$  = Velocity of air entering the chimney (m/s)

$A_c$  = Cross-section area of the chimney

$$= \pi r^2, \quad \text{where}$$

$r$  = radius of the chimney (m)

### 3.4.2. Pressure difference

The solar chimney is placed in the centre of the canopy area to generate the "sink effect" so that heated air may rise into it and escape from the top. The pressure difference between the pressure at the bottom and the top of the chimney is given by

$$P = (f_a - f_m) g H_c$$

where

$P$  = Pressure difference between the bottom and top of the chimney (Pa)

$g$  = Acceleration due to gravity ( $\text{m/s}^2$ )

$H_c$  = Height of the chimney (m)

### 3.4.3. Rotor power

The rising air imparts kinetic energy to a rotor placed in the chimney, causing it to rotate.

$$P_r = \eta_r \cdot (1/2) \int_m v^3 A_c$$

where  $P_r$  = Power the air turbine extracts from the rising air (W)

$\eta_r$  = power coefficient

### 3.4.4. Average output of a solar chimney power plant

Taking the physical parameters and the insolation at the site, the average output of the solar chimney power plant could be estimated using the formula,

$$P_a = \eta_c \cdot \eta_t \cdot (1-f) \cdot \frac{2 \cdot g \cdot H_c}{3 \cdot C_p \cdot T_a} \cdot F_c \cdot I$$

where,

$P_a$  = Average electrical output of the solar chimney power plant (W)

$\eta_c$  = Efficiency of the collector

$\eta_t$  = Efficiency of turbine and generator

(1-f) = Friction loss factor

$C_p$  = Specific heat capacity of air (J/KgoK)

$F_c$  = Area of the collector (m<sup>2</sup>)

$I$  = Solar Insolation at the site (W/m<sup>2</sup>)



### 3.4.5. Overall Efficiency of the Solar Chimney Power Plant

The overall efficiency of the solar chimney power plant is estimated as the ratio of the average output of the plant and the total solar insolation at the site.

Efficiency with which thermal power was converted to wind power is given by

$$\eta_w = \frac{A_c \cdot v \cdot \Delta p}{\dot{m} \cdot C_p \cdot (T_m - T_a)} = \frac{\Delta p}{\dot{m} \cdot C_p \cdot (T_m - T_a)}$$

The effect of side winds at the site was found to greatly influence the measured values of temperature and velocity. Provisions were made and the height at the periphery of the collector area was reduced to 10 cm. Some of the other defects like sagging of the transparent canopy, and tearing of certain spots in the canopy, were rectified.



Plate 1      Collector surface of the prototype  
SCPP at Tavanur



Plate 2      A view of the prototype SCPP  
at Tavanur





Plate 3

Suryamapi

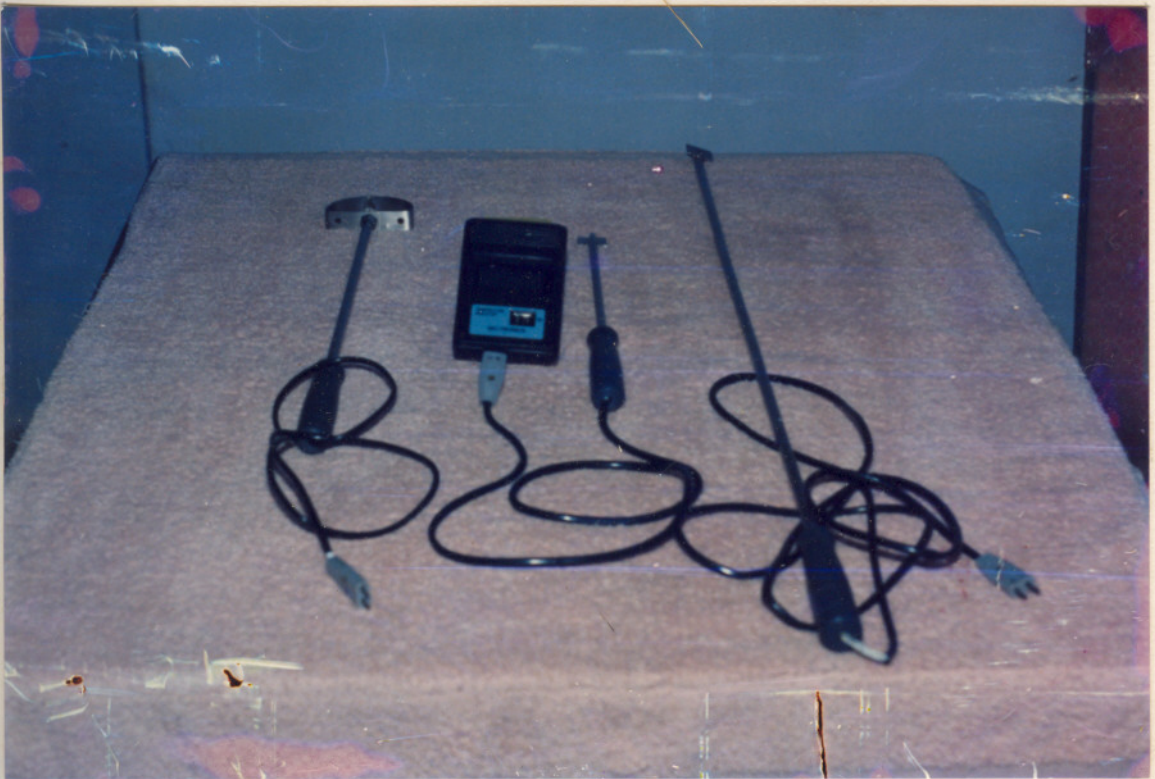


Plate 4

Digital temperature indicator



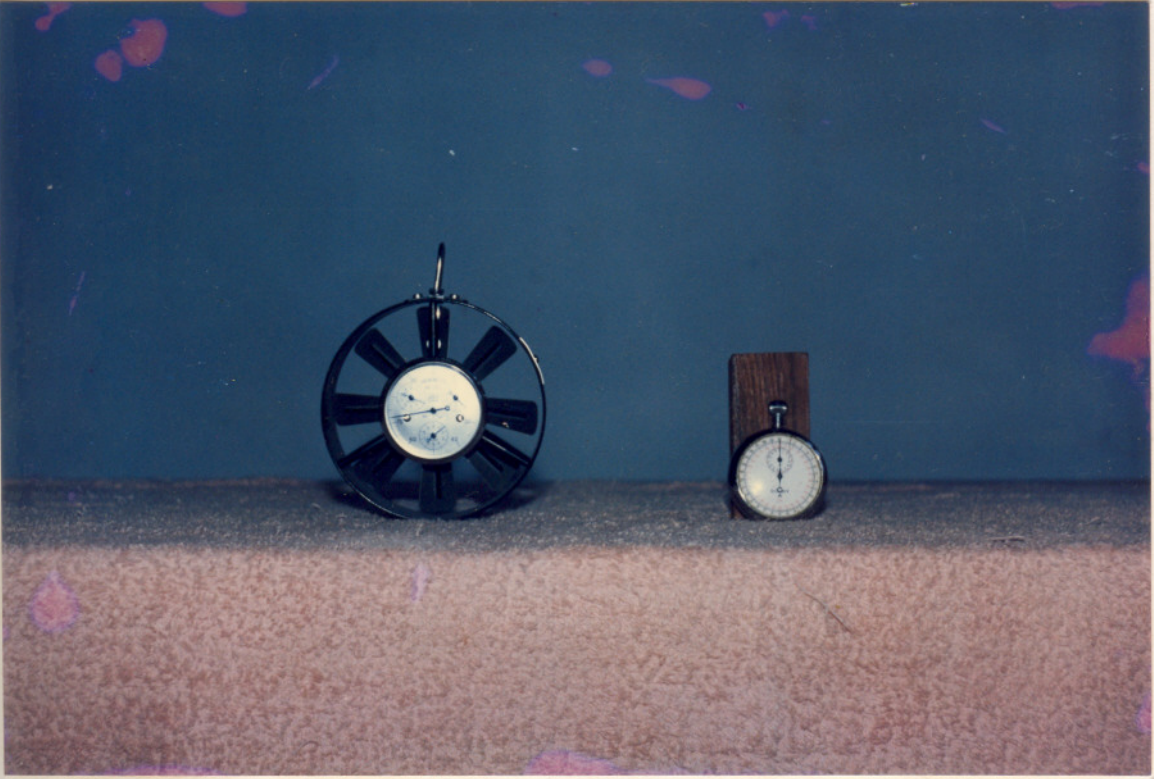


Plate 5

Vane anemometer



Plate 6

Electronic anemometer digital



## RESULTS AND DISCUSSION

The microscale prototype solar chimney plant was tested for six days and variations in ambient temperature, surface temperature and temperature of air at the inlet to the solar chimney with time was observed. Solar insolation and wind velocity at the entrance to the chimney, were also measured with reference to the time interval. Average output of the solar chimney power plant using Schlaich's equation was computed and compared with the actual power observed. The characteristics like mass flow rate of air and pressure difference between the top and bottom of the chimney were calculated from the data obtained from the plant. The mechanical efficiency of the plant, efficiency with which thermal power was converted to wind power and overall efficiency of the solar chimney plant were also obtained. These results are discussed in detail below.

### 4.1. Variation of temperature with time

The variations in ambient temperature, surface temperature and maximum temperature at the inlet to the chimney are displayed in tables 5 to 10 and in figures 6 to 11 respectively. On the first day, a maximum surface temperature of  $56^{\circ}\text{C}$  was attained and the temperature of air at the inlet

to the chimney reached a maximum of 47°C. The corresponding values for the second to the sixth day were 66°C and 50°C, 58°C and 49°C, 61°C and 48°C, 56°C and 47°C and 61°C and 45°C respectively. The average difference between the different parameters such as surface and ambient temperature, maximum and ambient temperature and surface and maximum temperature were obtained. These values were 18°C, 8.5°C and 9.5°C on the first day, 21°C, 13°C and 12°C on the second day and 20°C, 11°C and 9.3°C on the third day, with the remaining days showing almost the same trend. On a particular day the values of temperature difference obtained from the Manzanares experimental station were 46°C, 21°C and 25°C respectively. The shady nature of the location where the plant was constructed and the constraints which presented themselves at the time of tests could have caused this reduction in the values.

#### 4.2. Variation of insolation and air velocity with time

The variations in insolation and measured air velocity with time are displayed in tables 11 to 16 and in figures 12 to 17 respectively. A maximum air velocity at the chimney entrance of 2.47 m/s was obtained at the insolation level of 650 W/m<sup>2</sup> on the first day. The effect of outside wind at the site was very high on the first day and this affected



Table 5. Variation of temperature with time

Date 07/10/'93	Time (h)			
	12.00	12.30	13.00	13.30
Ta (°C)	35	36	33	32
Tm (°C)	46	47	39	38
Ts (°C)	54	56	50	48

Ta - Ambient temperature

Tm - Temperature of air at the inlet to the chimney

Ts - Surface temperature

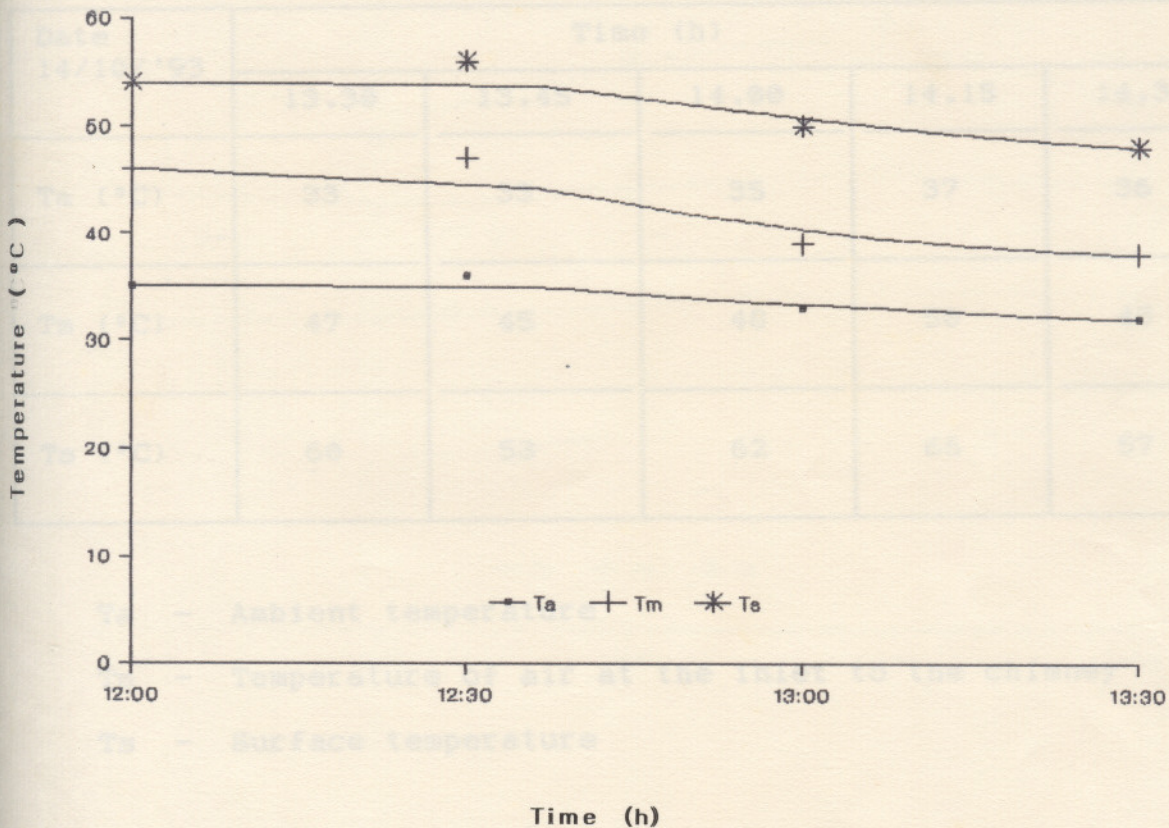


Fig.6 Graph showing variation of temperature with time



**Table 6. Variation of temperature with time**

Date 14/10/'93	Time (h)				
	13.30	13.45	14.00	14.15	14.30
Ta (°C)	33	33	35	37	36
Tm (°C)	47	45	48	50	48
Ts (°C)	60	53	62	66	57

Ta - Ambient temperature

Tm - Temperature of air at the inlet to the chimney

Ts - Surface temperature

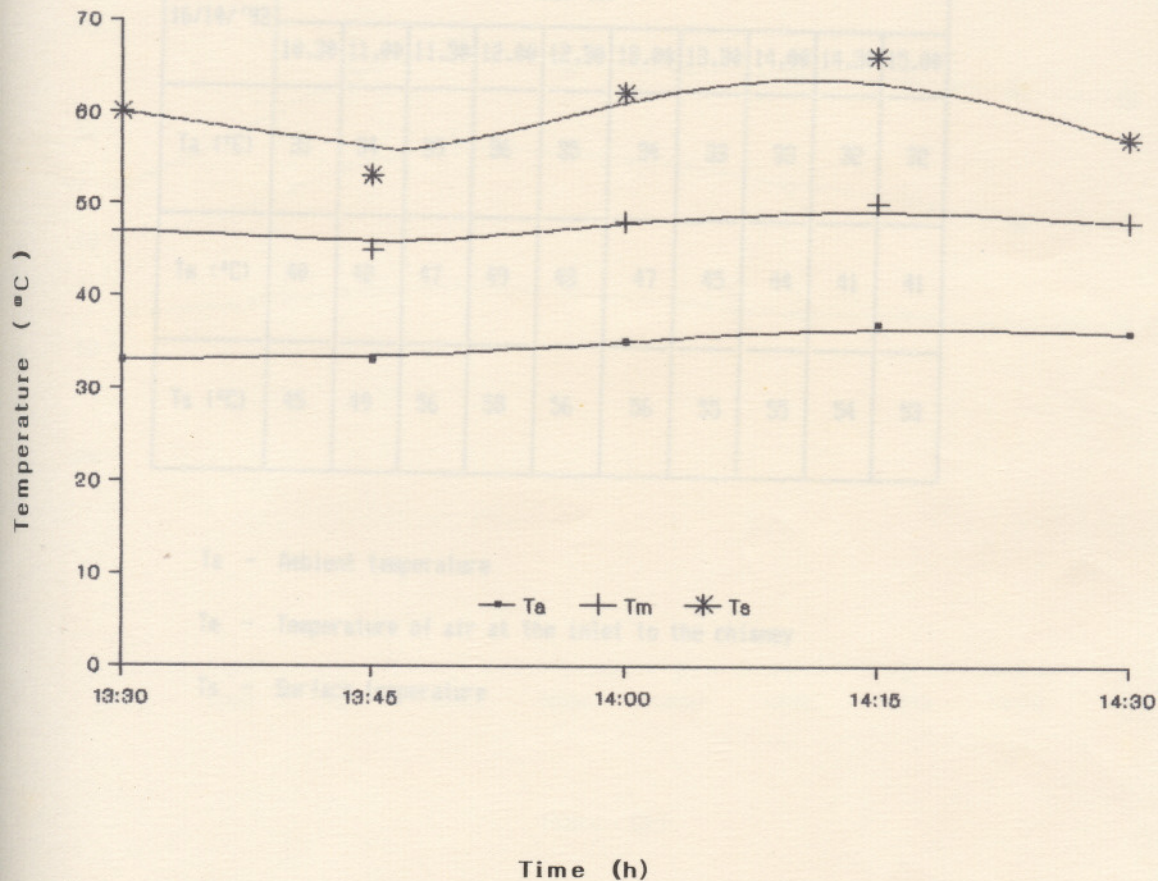


Fig.7 Graph showing variation of temperature with time



Table 7. Variation of temperature with time

Date 16/10/'93	Time (h)									
	10.30	11.00	11.30	12.00	12.30	13.00	13.30	14.00	14.30	15.00
T <sub>a</sub> (°C)	33	34	35	36	35	34	33	33	32	32
T <sub>m</sub> (°C)	40	42	47	49	48	47	45	44	41	41
T <sub>s</sub> (°C)	45	49	56	58	56	56	55	55	54	53

T<sub>a</sub> - Ambient temperature

T<sub>m</sub> - Temperature of air at the inlet to the chimney

T<sub>s</sub> - Surface temperature

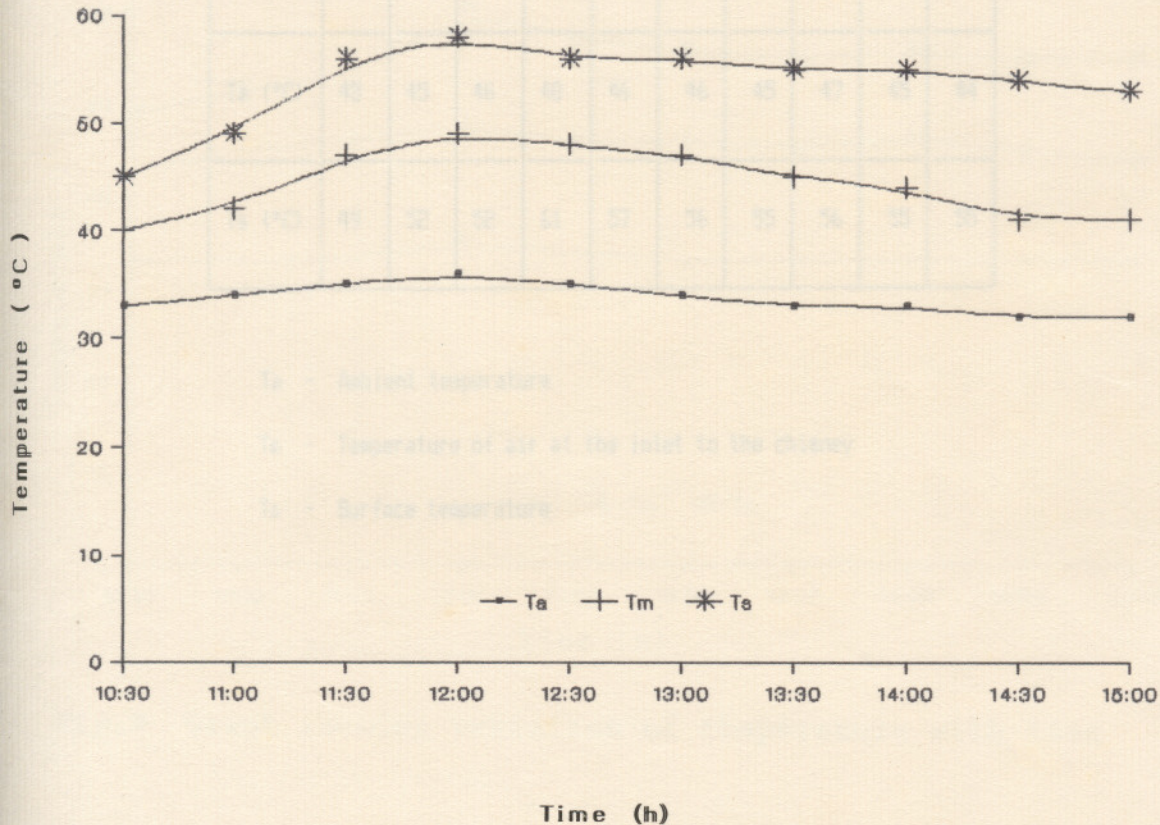


Fig.8 Graph showing variation of temperature with time



Table 8. Variation of temperature with time

Date 31/10/'93	Time (h)									
	10.30	11.00	11.30	12.00	12.30	13.00	13.30	14.00	14.30	15.00
T <sub>a</sub> (°C)	33	33	33	35	34	33	33	33	33	33
T <sub>m</sub> (°C)	43	45	46	48	46	46	45	47	45	44
T <sub>s</sub> (°C)	49	52	52	61	57	56	55	56	55	55

T<sub>a</sub> - Ambient temperature

T<sub>m</sub> - Temperature of air at the inlet to the chimney

T<sub>s</sub> - Surface temperature

Table 9. Variation of temperature with time

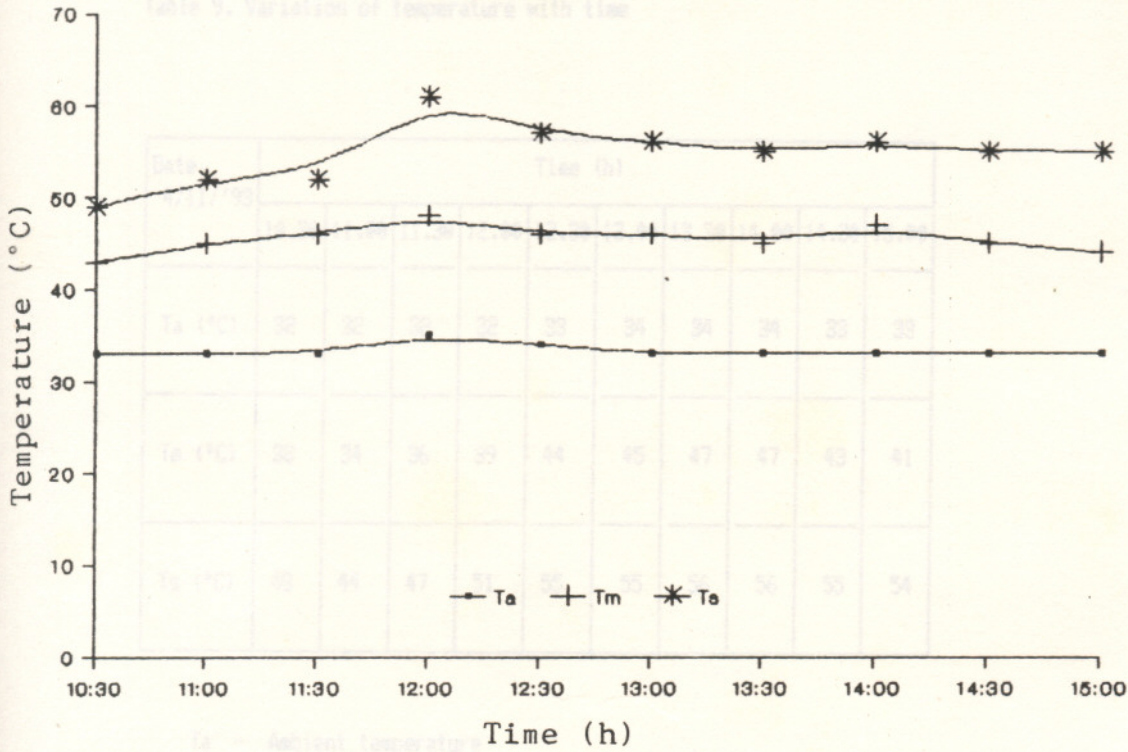


Fig.9 Graph showing variation of temperature with time



Table 9. Variation of temperature with time

Date 4/11/'93	Time (h)									
	10.30	11.00	11.30	12.00	12.30	13.00	13.30	14.00	14.30	15.00
Ta (°C)	32	32	32	32	33	34	34	34	33	33
Tm (°C)	38	34	36	39	44	45	47	47	43	41
Ts (°C)	48	44	47	51	55	55	56	56	55	54

Ta - Ambient temperature

Tm - Temperature of air at the inlet to the chimney

Ts - Surface temperature

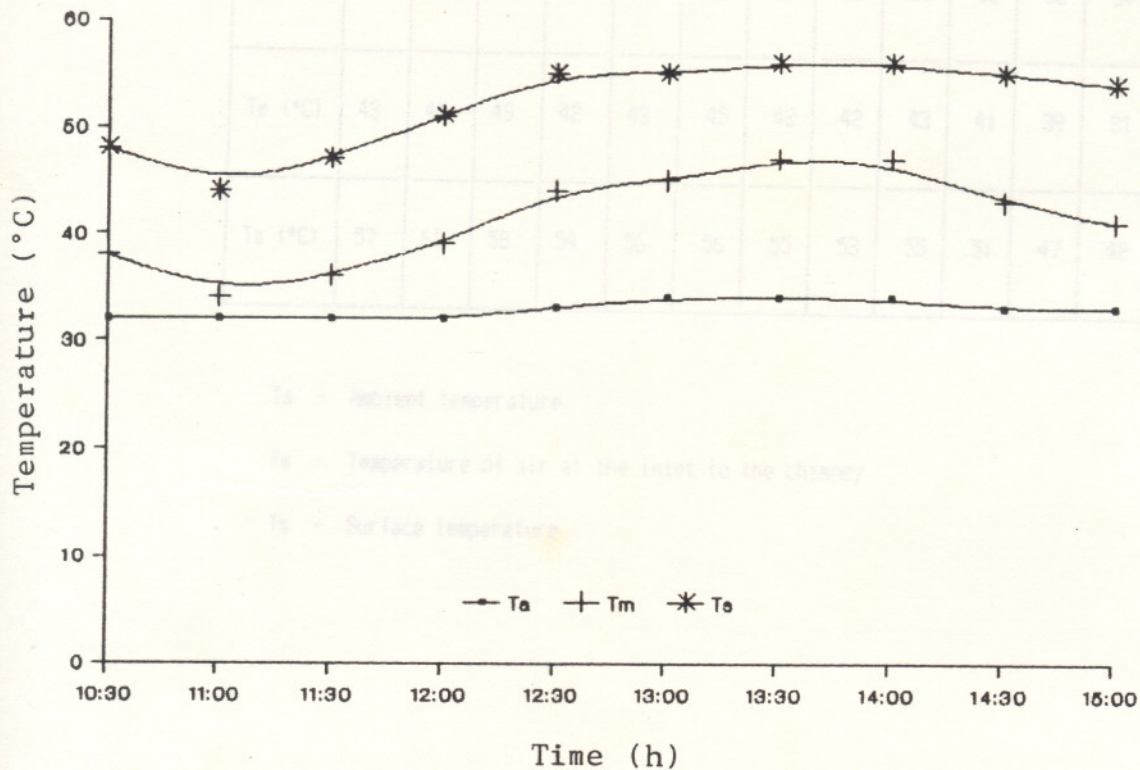


Fig.10 Graph showing variation of temperature with time



Table 10. Variation of temperature with time

Date 5/11/'93	Time (h)											
	12.00	12.30	13.00	13.30	14.00	14.30	15.00	15.30	16.00	16.30	17.00	17.30
T <sub>a</sub> (°C)	34	34	34	34	34	33	33	33	33	32	32	30
T <sub>m</sub> (°C)	43	44	43	42	43	45	43	42	43	41	39	31
T <sub>s</sub> (°C)	57	61	58	54	56	56	55	53	55	51	47	42

T<sub>a</sub> - Ambient temperature

T<sub>m</sub> - Temperature of air at the inlet to the chimney

T<sub>s</sub> - Surface temperature

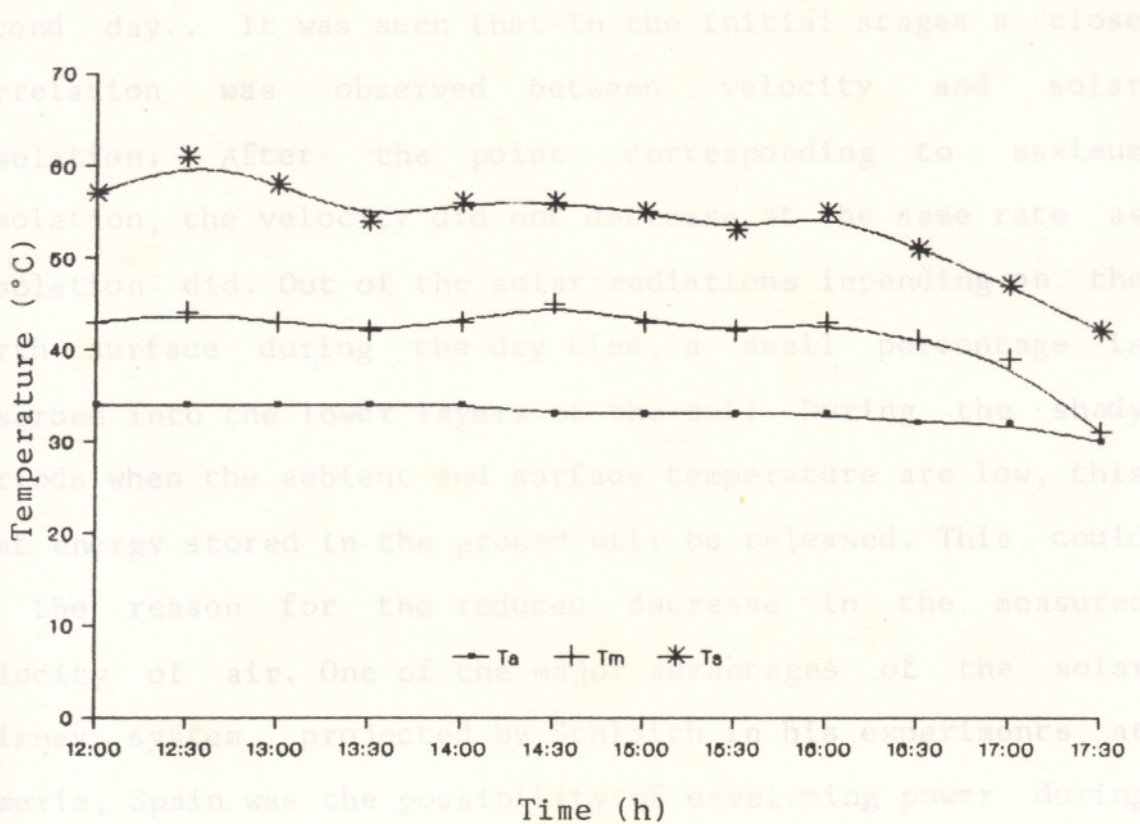


**Fig.11** Graph showing variation of temperature with time



the velocity of air flow inside the chimney. During the remaining days, the maximum air velocity observed was 2.45 m/s inside the chimney at an insolation level of  $1000 \text{ W/m}^2$  on the second day.. It was seen that in the initial stages a close correlation was observed between velocity and solar insolation. After the point corresponding to maximum insolation, the velocity did not decrease at the same rate as insolation did. Out of the solar radiations impinging on the earth surface during the day time, a small percentage is absorbed into the lower layers of the soil. During the shady periods when the ambient and surface temperature are low, this heat energy stored in the ground will be released. This could be the reason for the reduced decrease in the measured velocity of air. One of the major advantages of the solar chimney system, projected by Schlaich in his experiments at Almeria, Spain was the possibility of developing power during shady periods - even during the night. The results observed at Manzanares facility and Tavanur prototype were found matching in this regard.

#### 4.3. Variation of theoretical and observed power with insolation and time

The variation of theoretical and observed power output with insolation and time are displayed in tables 17 to 22 and in figures 18 to 23 respectively. The average expected

Table 11. Variation of velocity and insolation with time

Date 07/10/'93	Time (h)			
	12.00	12.30	13.00	13.30
Velocity (m/s)	2.32	2.47	1.89	2.33
Insolation <sup>2</sup> (W/m <sup>2</sup> )	500	650	500	400

Fig. 12. Graph showing variation of velocity and insolation with time



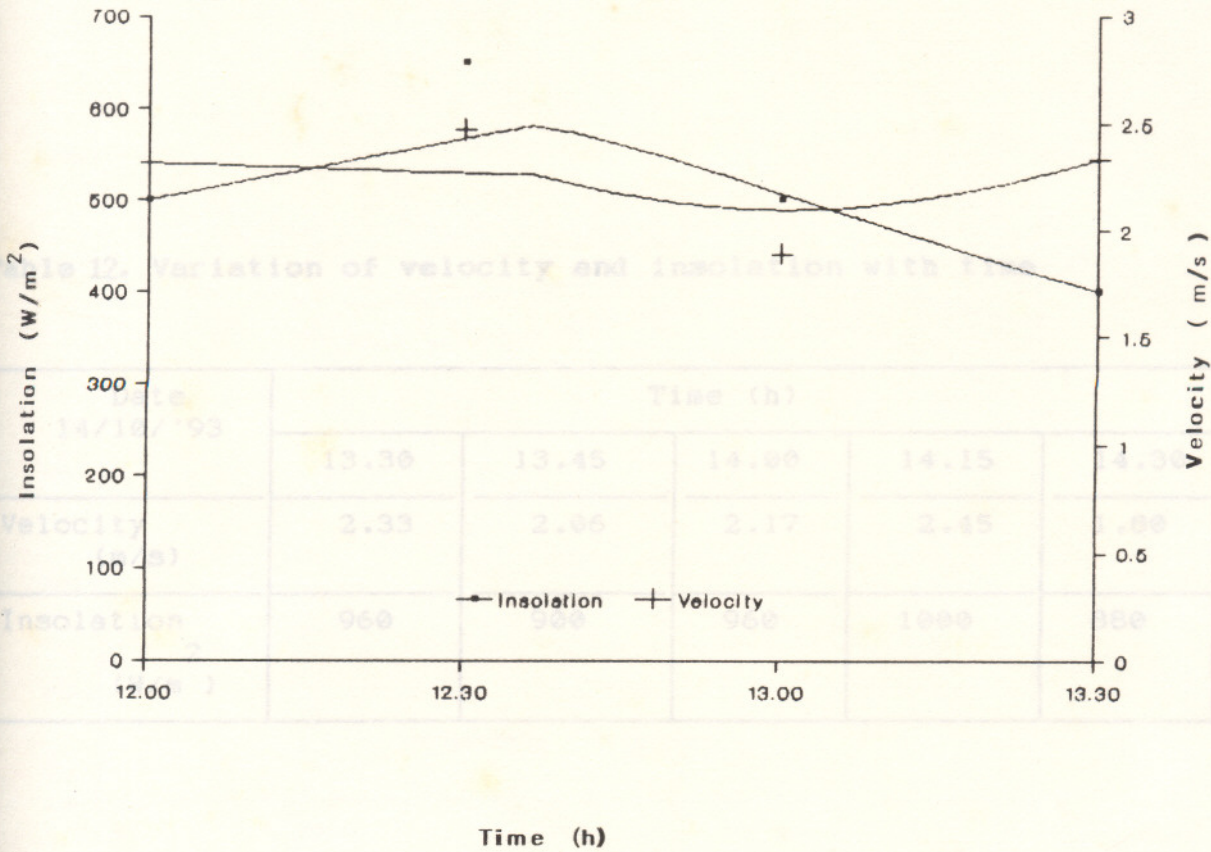


Fig.12 Graph showing variation of velocity and insolation with time

Table 12. Variation of velocity and insolation with time

Date 14/10/'93	Time (h)				
	13.30	13.45	14.00	14.15	14.30
Velocity (m/s)	2.33	2.06	2.17	2.45	1.80
Insolation <sup>2</sup> (W/m <sup>2</sup> )	960	900	960	1000	880



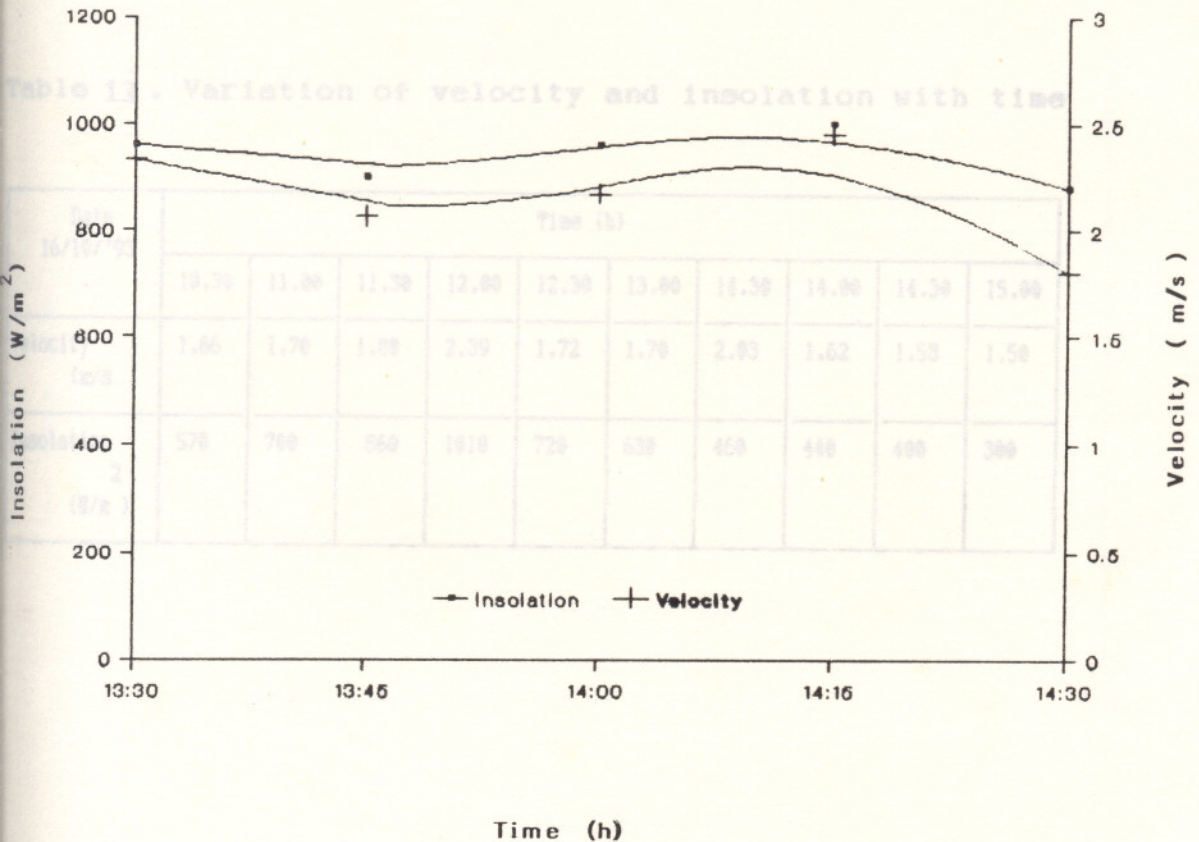


Fig.13 Graph showing variation of velocity and insolation with time

Table 13 . Variation of velocity and insolation with time

Date 16/10/'93	Time (h)									
	10.30	11.00	11.30	12.00	12.30	13.00	14.30	14.00	14.30	15.00
Velocity (m/s)	1.66	1.70	1.80	2.39	1.72	1.70	2.03	1.62	1.58	1.50
Insolation 2 (W/m)	570	700	860	1010	720	630	460	440	400	300



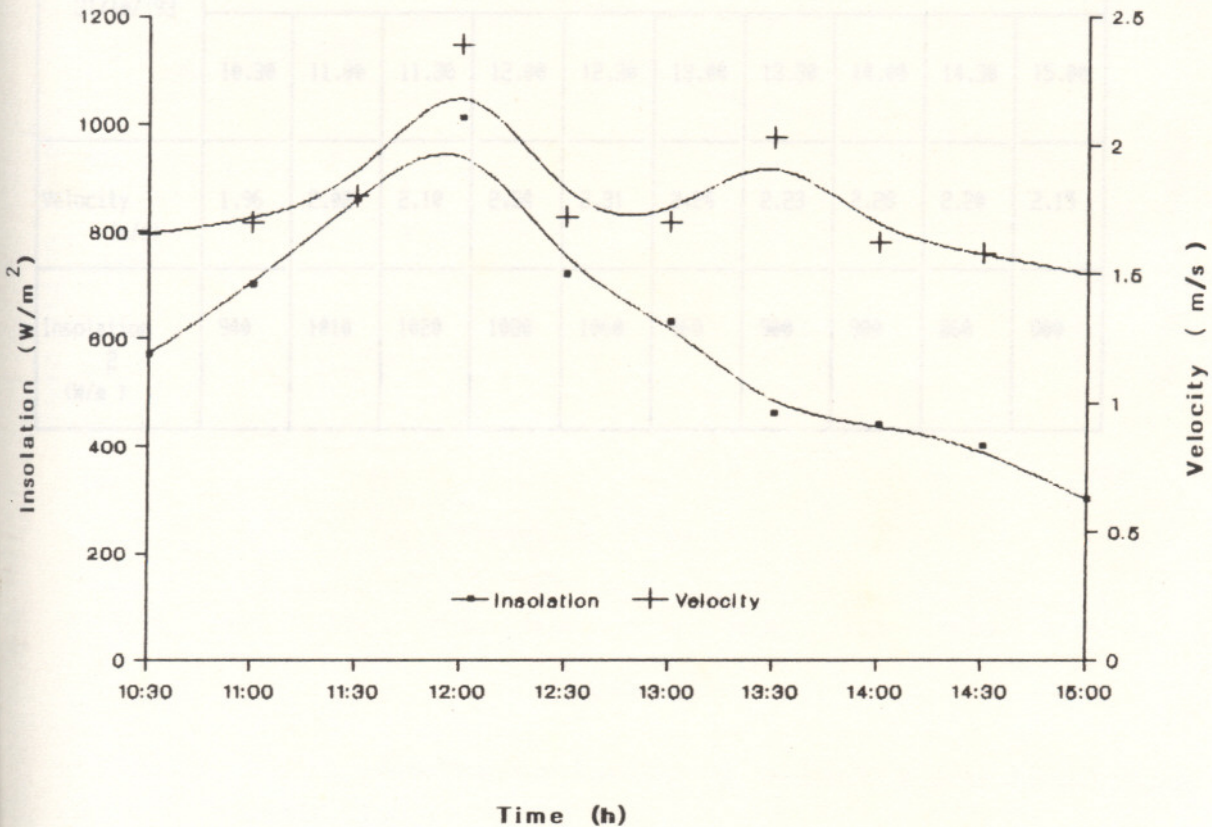


Fig.14 Graph showing variation of velocity and insolation with time

Table 14. Variation of velocity and insolation with time

Date 31/10/'93	Time (h)									
	10.30	11.00	11.30	12.00	12.30	13.00	13.30	14.00	14.30	15.00
Velocity (m/s)	1.96	2.02	2.10	2.34	2.31	2.24	2.23	2.28	2.20	2.15
Insolation 2 (W/m )	940	1010	1020	1080	1060	960	900	900	860	800



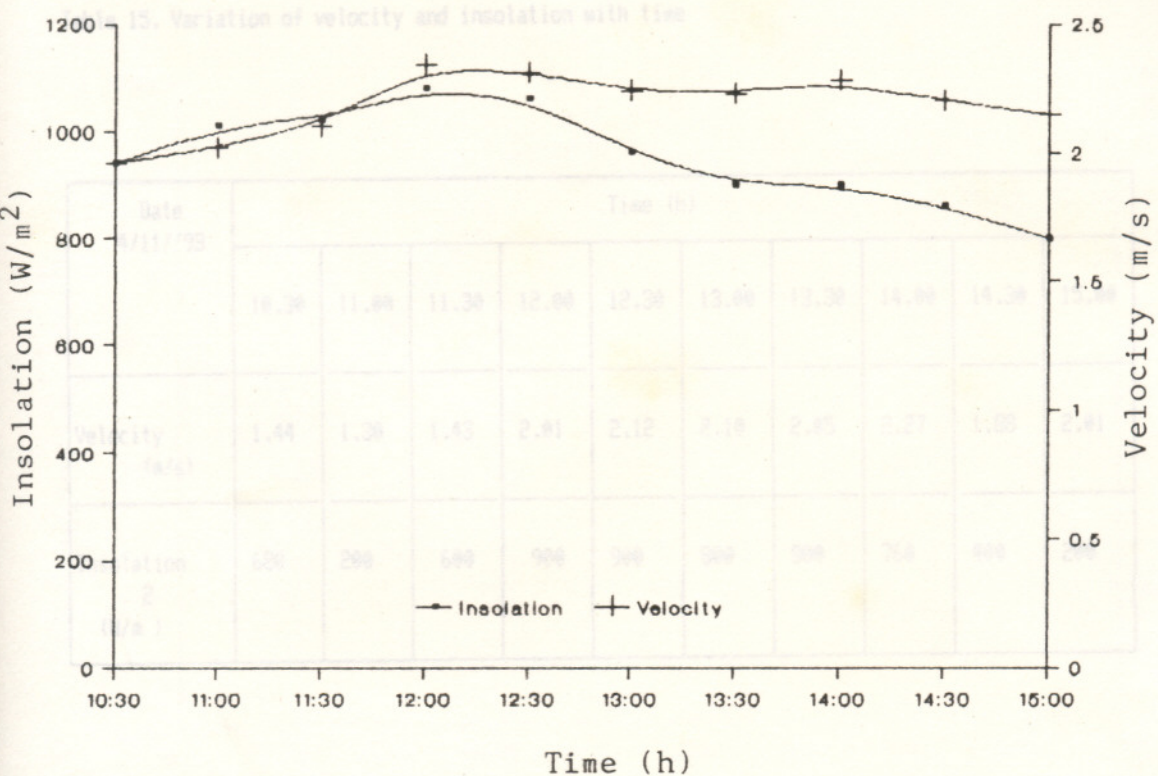


Fig.15 Graph showing variation of velocity and insolation with time

Table 15. Variation of velocity and insolation with time

Date 4/11/'93	Time (h)									
	10.30	11.00	11.30	12.00	12.30	13.00	13.30	14.00	14.30	15.00
Velocity (m/s)	1.44	1.30	1.43	2.01	2.12	2.10	2.05	2.27	1.88	2.01
Insolation 2 (W/m)	680	200	600	900	900	800	800	760	400	200



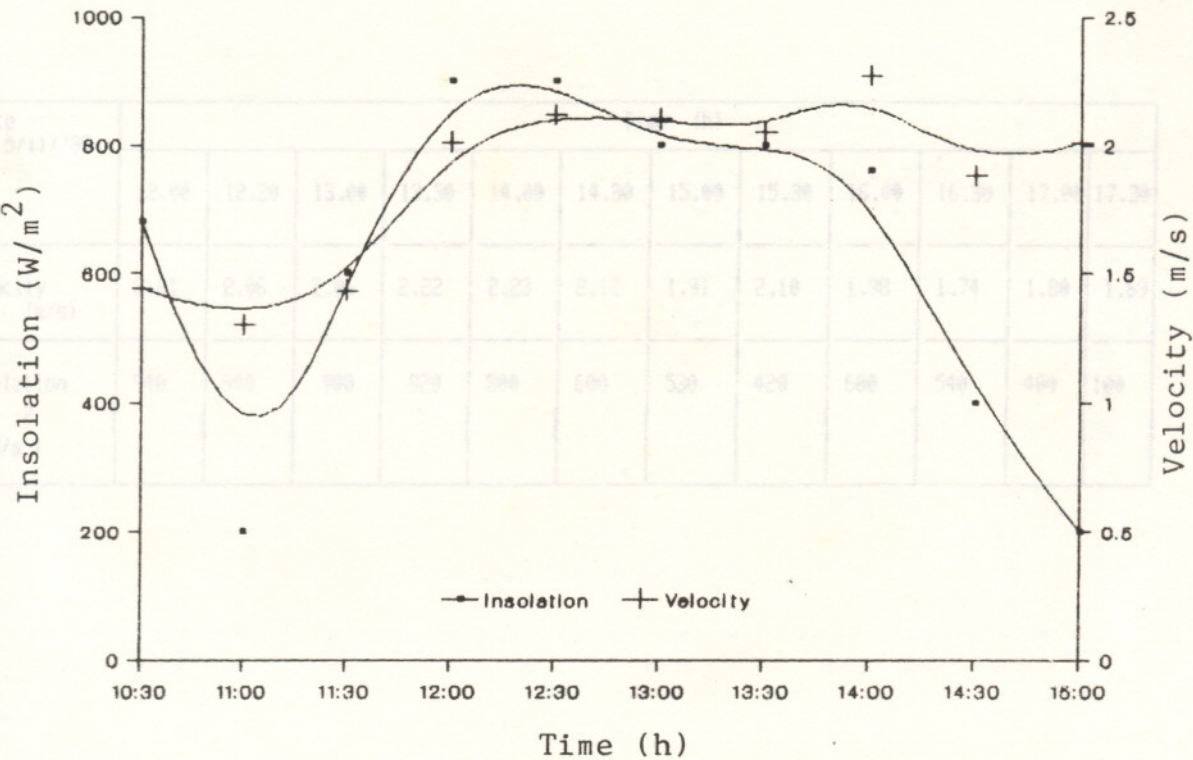


Fig.16 Graph showing variation of velocity and insolation with time

Table 16. Variation of velocity and insolation with time

Date 5/11/'93	Time (h)											
	12.00	12.30	13.00	13.30	14.00	14.30	15.00	15.30	16.00	16.30	17.00	17.30
Velocity (m/s)	2.21	2.06	2.06	2.22	2.23	2.12	1.91	2.10	1.98	1.74	1.80	1.69
Insolation 2 (W/m)	940	940	900	820	800	600	530	420	600	540	400	100



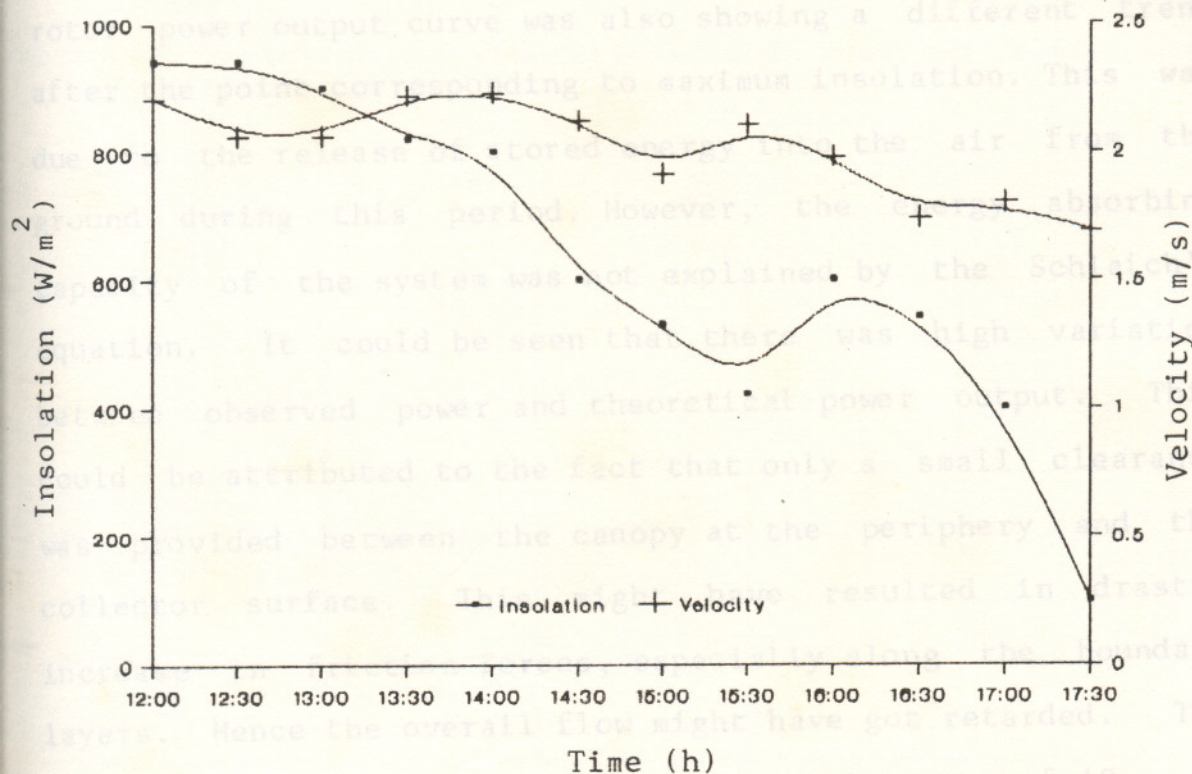


Fig.17 Graph showing variation of velocity and insolation with time

power output from the solar chimney plant using Schlaich's equation was found to closely match with insolation. This is justified as the most prominent variable in the Schlaich's equation was insolation. Similar to the velocity curve, the rotor power output curve was also showing a different trend after the point corresponding to maximum insolation. This was due to the release of stored energy into the air from the ground during this period. However, the energy absorbing capacity of the system was not explained by the Schlaich's equation. It could be seen that there was high variation between observed power and theoretical power output. This could be attributed to the fact that only a small clearance was provided between the canopy at the periphery and the collector surface. This might have resulted in drastic increase in friction forces, especially along the boundary layers. Hence the overall flow might have got retarded. The canopy gap could not be increased beyond the range of 10 - 15 cm, as the side winds at the location pumped the heated air out of the plant instead of forcing it up through the chimney at larger canopy gap at the periphery. This is a major limitation of plants having small dimensions. In the power plant at Almeria, Spain, the collector area was very large and the height of the canopy above the ground surface was about 2m. The friction losses will be much reduced in this case and



Table 17. Variation of theoretical and observed power with insolation and time

Date 07/10/'93	Time (h)			
	12.00	12.30	13.00	13.30
Rotor power (W)	0.170	0.204	0.094	0.1762
Expected Average output of SCPP (W)	0.776	1.005	0.781	0.627
Insolation 2 (W/m )	500	650	500	400

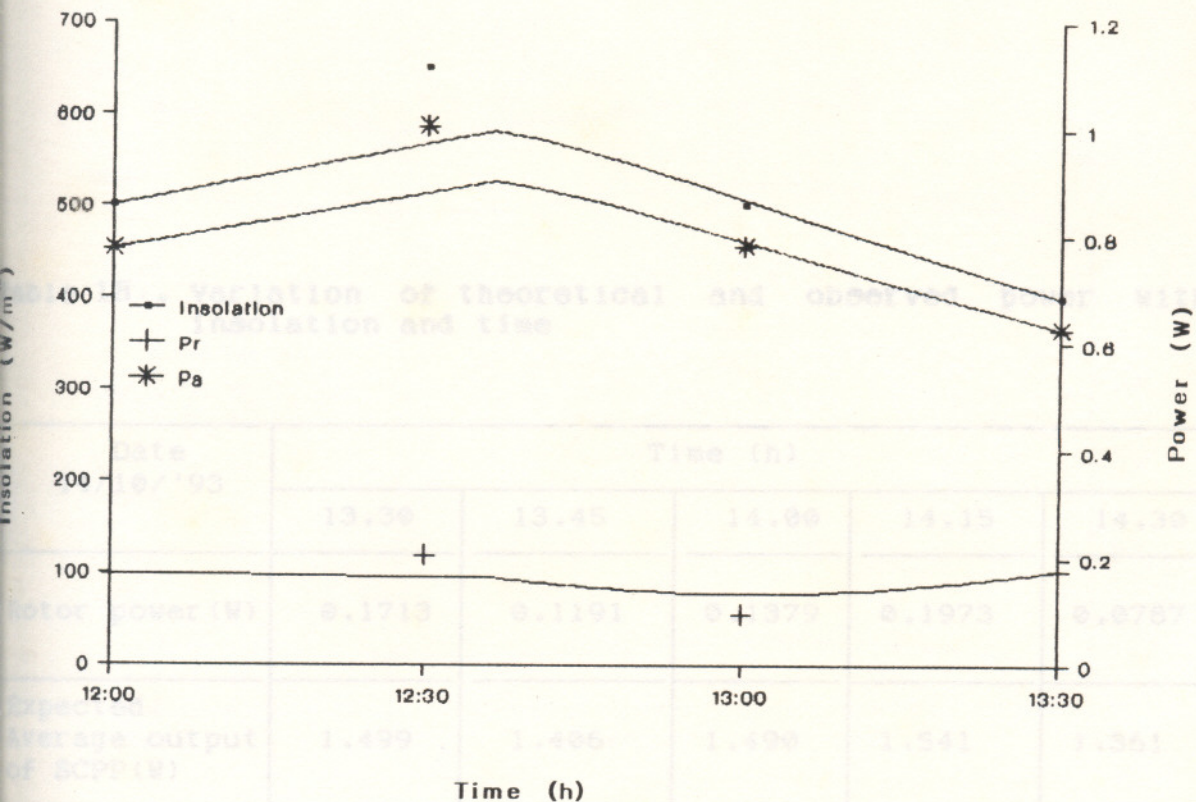


Fig.18 Graph showing variation of theoretical and observed power with insolation and time



Table 18. Variation of theoretical and observed power with insolation and time

Date 14/10/'93	Time (h)				
	13.30	13.45	14.00	14.15	14.30
Rotor power (W)	0.1713	0.1191	0.1379	0.1973	0.0787
Expected Average output of SCPP (W)	1.499	1.406	1.490	1.541	1.361
Insolation <sup>2</sup> (W/m <sup>2</sup> )	960	900	960	1000	880

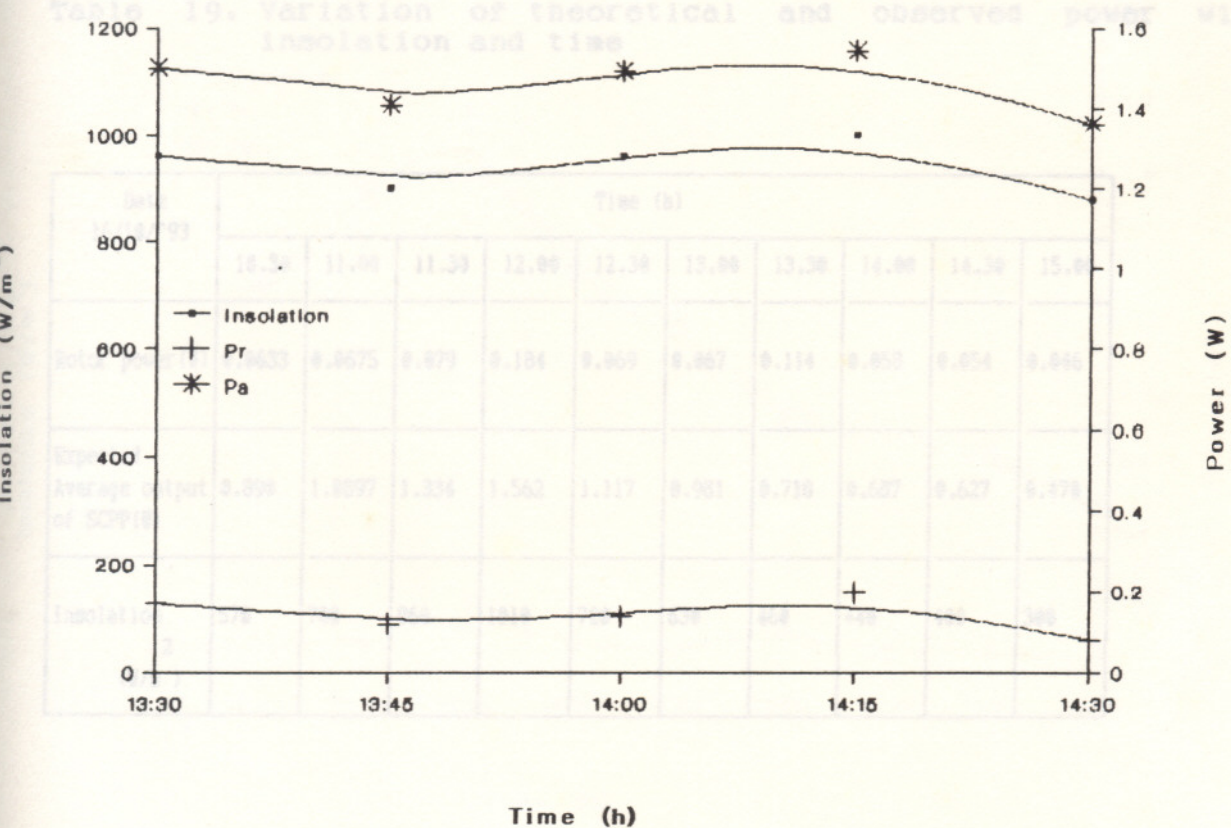


Fig.19 Graph showing variation of theoretical and observed power with insolation and time



Table 19. Variation of theoretical and observed power with insolation and time

Date 16/10/'93	Time (h)									
	10.30	11.00	11.30	12.00	12.30	13.00	13.30	14.00	14.30	15.00
Rotor power (W)	0.0633	0.0675	0.079	0.184	0.069	0.067	0.114	0.058	0.054	0.046
Expected Average output of SCPP (W)	0.890	1.0097	1.334	1.562	1.117	0.981	0.718	0.687	0.627	0.470
Insolation 2 (W/m)	570	700	860	1010	720	630	460	440	400	300

Table 25. Variation of theoretical and observed power with insolation and time

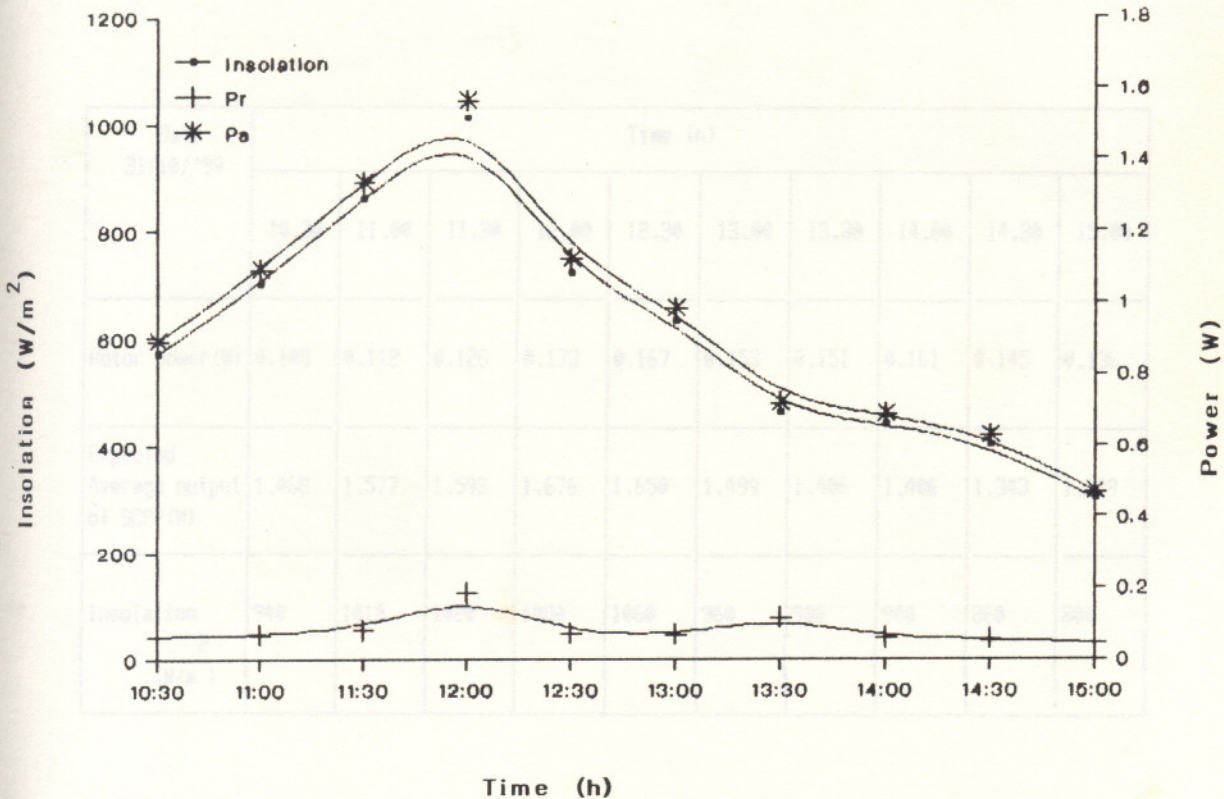


Fig.20 Graph showing variation of theoretical and observed power with insolation and time



Table 20. Variation of theoretical and observed power with insolation and time

Date 31/10/'93	Time (h)									
	10.30	11.00	11.30	12.00	12.30	13.00	13.30	14.00	14.30	15.00
Rotor power (W)	0.103	0.112	0.126	0.173	0.167	0.153	0.151	0.161	0.145	0.136
Expected Average output of SCPF (W)	1.468	1.577	1.593	1.676	1.650	1.499	1.406	1.406	1.343	1.249
Insolation 2 (W/m)	940	1010	1020	1080	1060	960	900	900	860	800

Fig.21 Graph showing variation of theoretical and

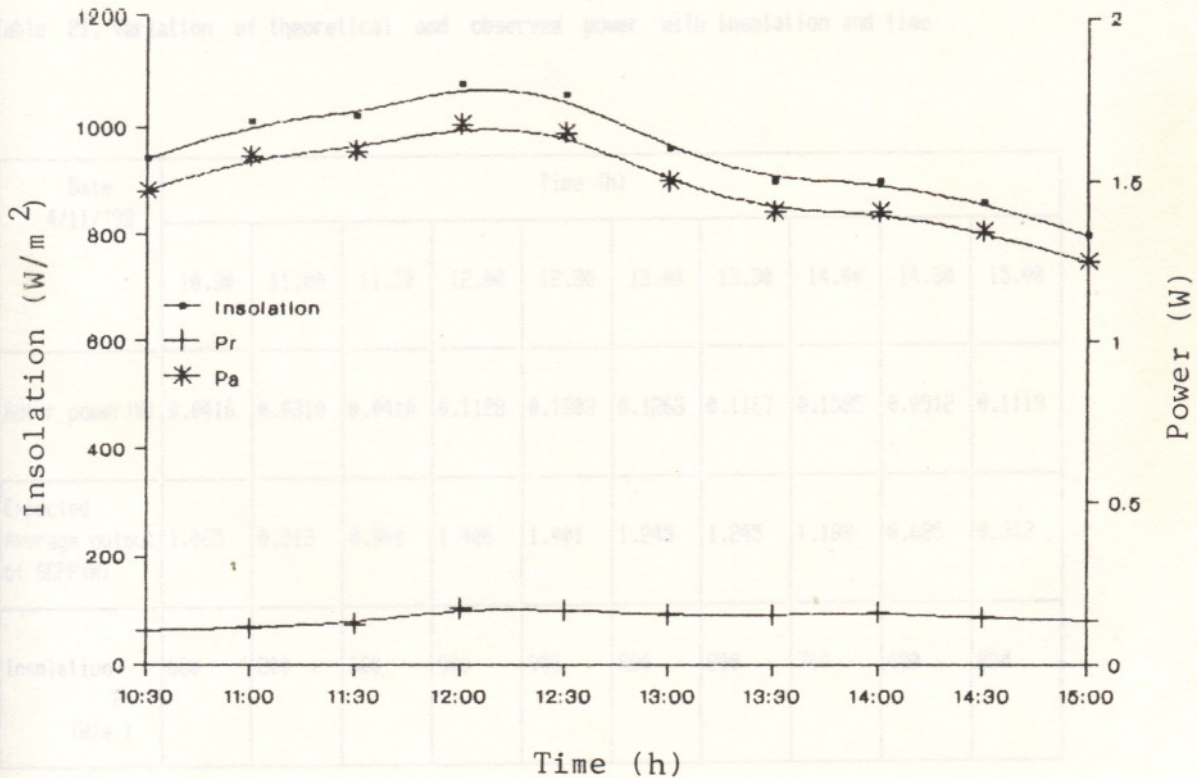


Fig.21 Graph showing variation of theoretical and observed power with insolation and time



Table 21. Variation of theoretical and observed power with insolation and time

Date 4/11/'93	Time (h)									
	10.30	11.00	11.30	12.00	12.30	13.00	13.30	14.00	14.30	15.00
Rotor power (W)	0.0416	0.0310	0.0410	0.1128	0.1303	0.1263	0.1167	0.1585	0.0912	0.1119
Expected Average output of SCPP (W)	1.065	0.313	0.940	1.406	1.401	1.245	1.245	1.183	0.625	0.312
Insolation 2 (W/m)	680	200	600	900	900	800	800	760	400	200

Fig. 22. Graph showing variation of theoretical and

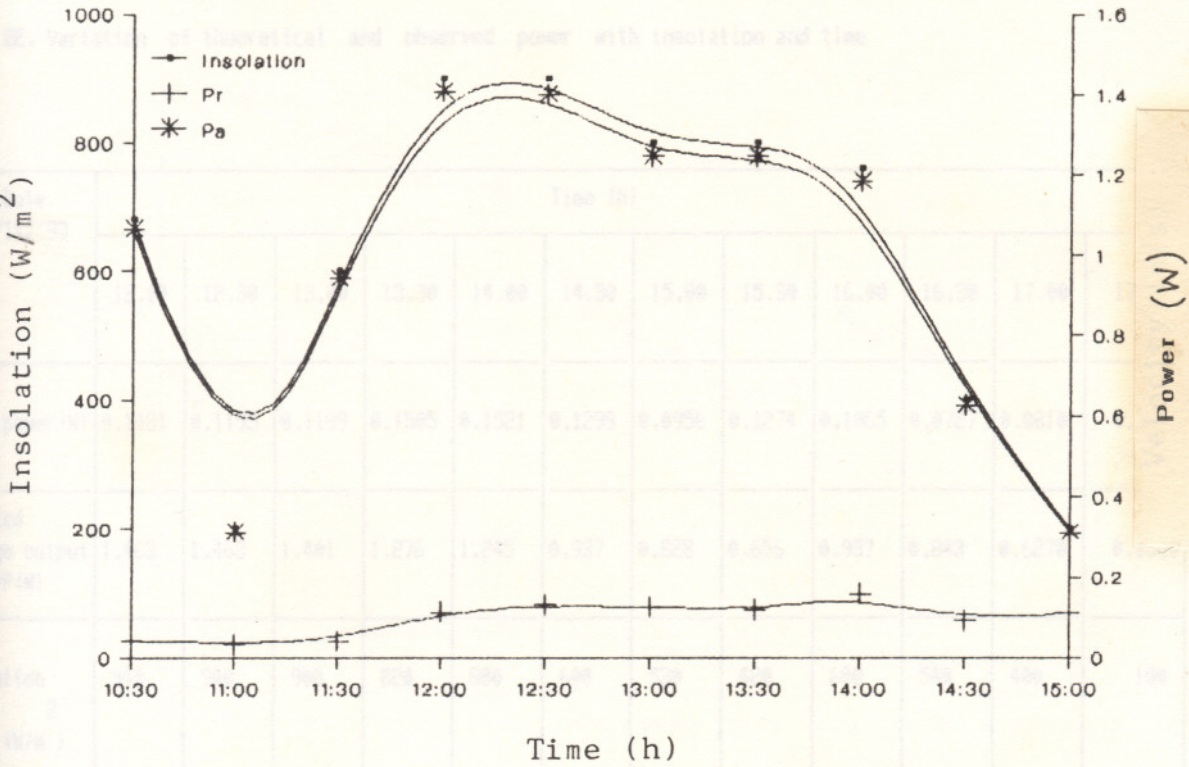


Fig.22 Graph showing variation of theoretical and observed power with insolation and time



le 22. Variation of theoretical and observed power with insolation and time

Date	Time (h)											
	12.00	12.30	13.00	13.30	14.00	14.30	15.00	15.30	16.00	16.30	17.00	17.30
Observed power (W)	0.1481	0.1195	0.1199	0.1505	0.1521	0.1299	0.0956	0.1274	0.1065	0.0727	0.0810	0.0688
Expected average output SCPP (W)	1.463	1.463	1.401	1.276	1.245	0.937	0.828	0.656	0.937	0.843	0.6270	0.1580
Insolation $I_p$ (W/m <sup>2</sup> )	940	940	900	820	800	600	530	420	600	540	400	100

Fig.23 Graph showing variation of theoretical and observed power with insolation and time

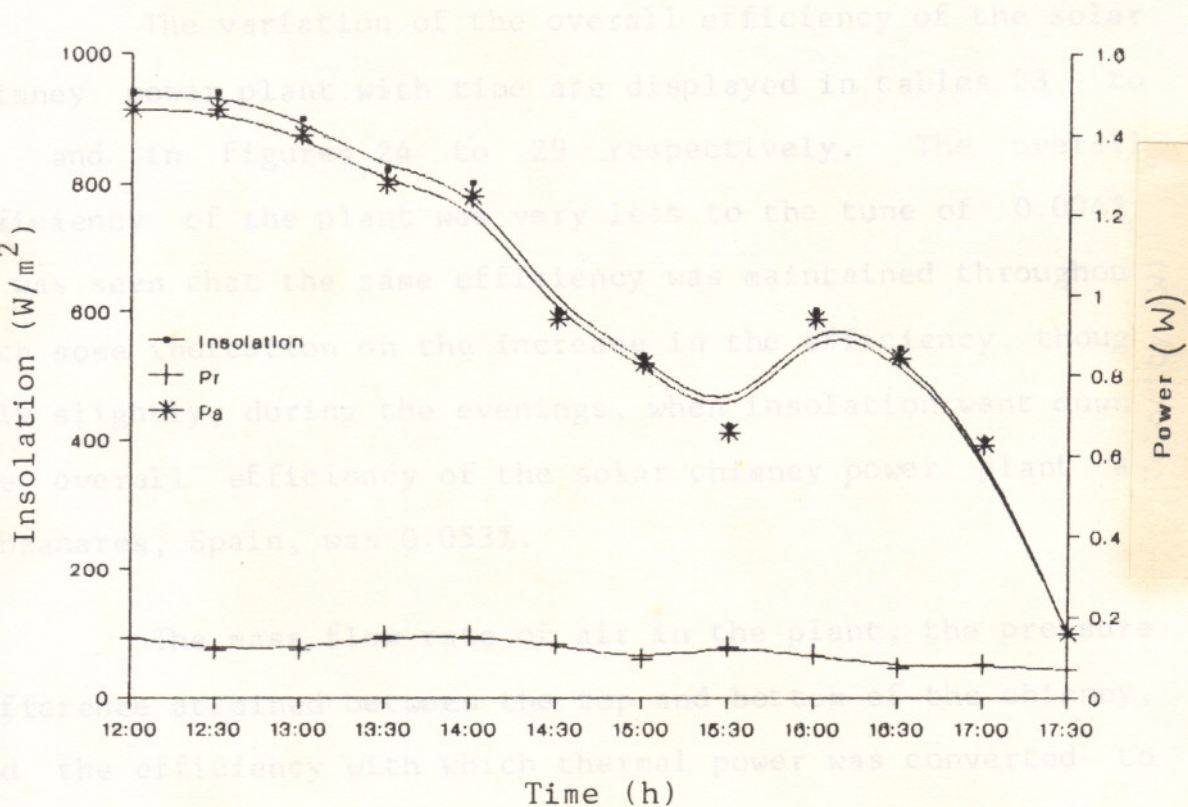


Fig.23 Graph showing variation of theoretical and observed power with insolation and time



hence the higher average expected output of the solar chimney power plant using Schlaich's equation.

#### 4.4. Overall efficiency

The variation of the overall efficiency of the solar chimney power plant with time are displayed in tables 23 to 28 and in figures 24 to 29 respectively. The overall efficiency of the plant was very less to the tune of 0.004%. It was seen that the same efficiency was maintained throughout with some indication on the increase in the efficiency, though only slightly, during the evenings, when insolation went down. The overall efficiency of the solar chimney power plant at Manzanares, Spain, was 0.053%.

The mass flow rate of air in the plant, the pressure difference attained between the top and bottom of the chimney, and the efficiency with which thermal power was converted to wind power were also calculated and the results are tabulated in appendices III, IV, V, VI, VII & VIII.

Table 23. Variation of overall efficiency with time

Date 07/10/'93	Time (h)			
	12.00	12.30	13.00	13.30
Overall Efficiency (%)	0.0043	0.0043	0.0043	0.0043

Table 24. Variation of overall efficiency with time

Date 14/10/'93	Time (h)				
	13.30	13.45	14.00	14.15	14.30
Overall Efficiency (%)	0.0043	0.0043	0.0043	0.0043	0.0043



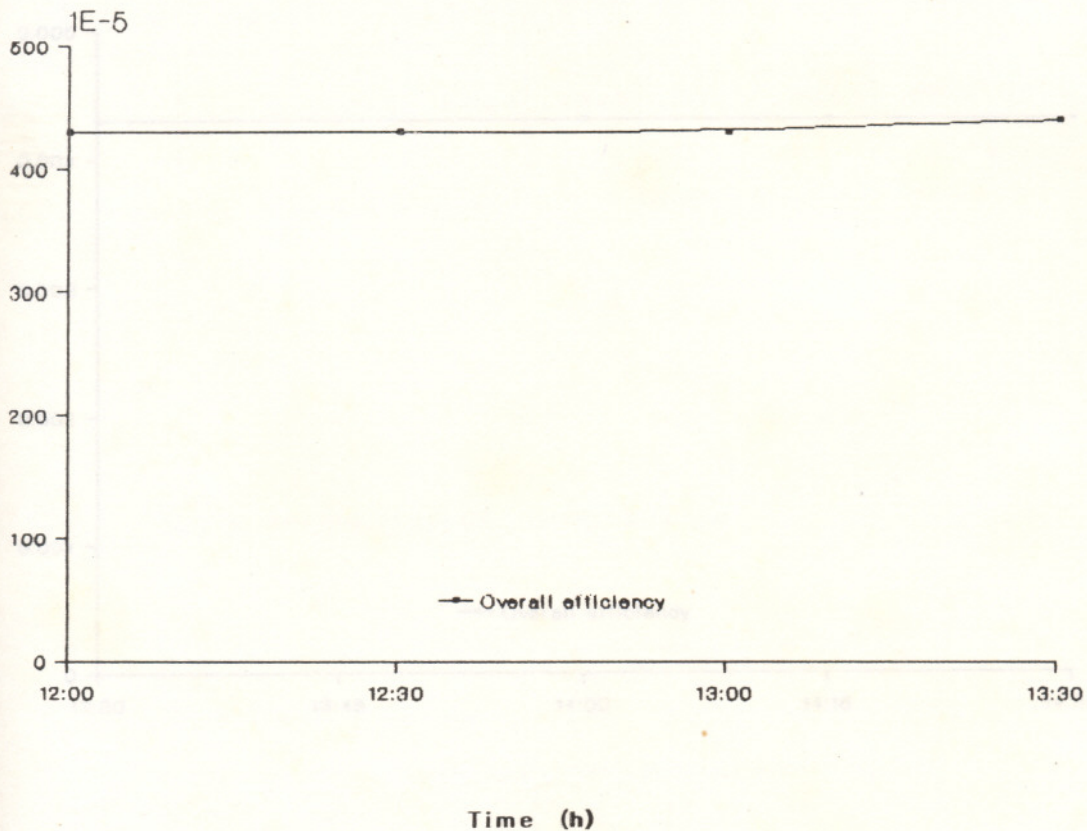


Fig.24 Graph showing variation of overall efficiency with time

Efficiency ( % )

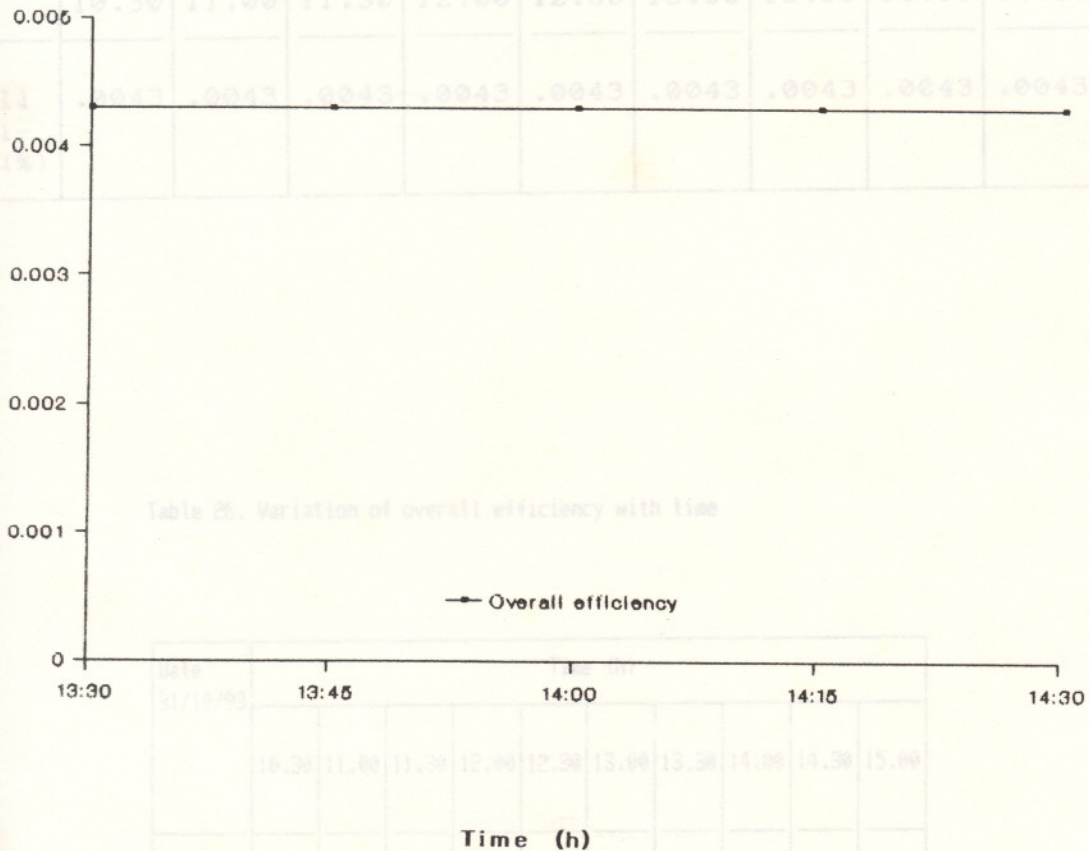


Fig.25 Graph showing variation of overall efficiency with time





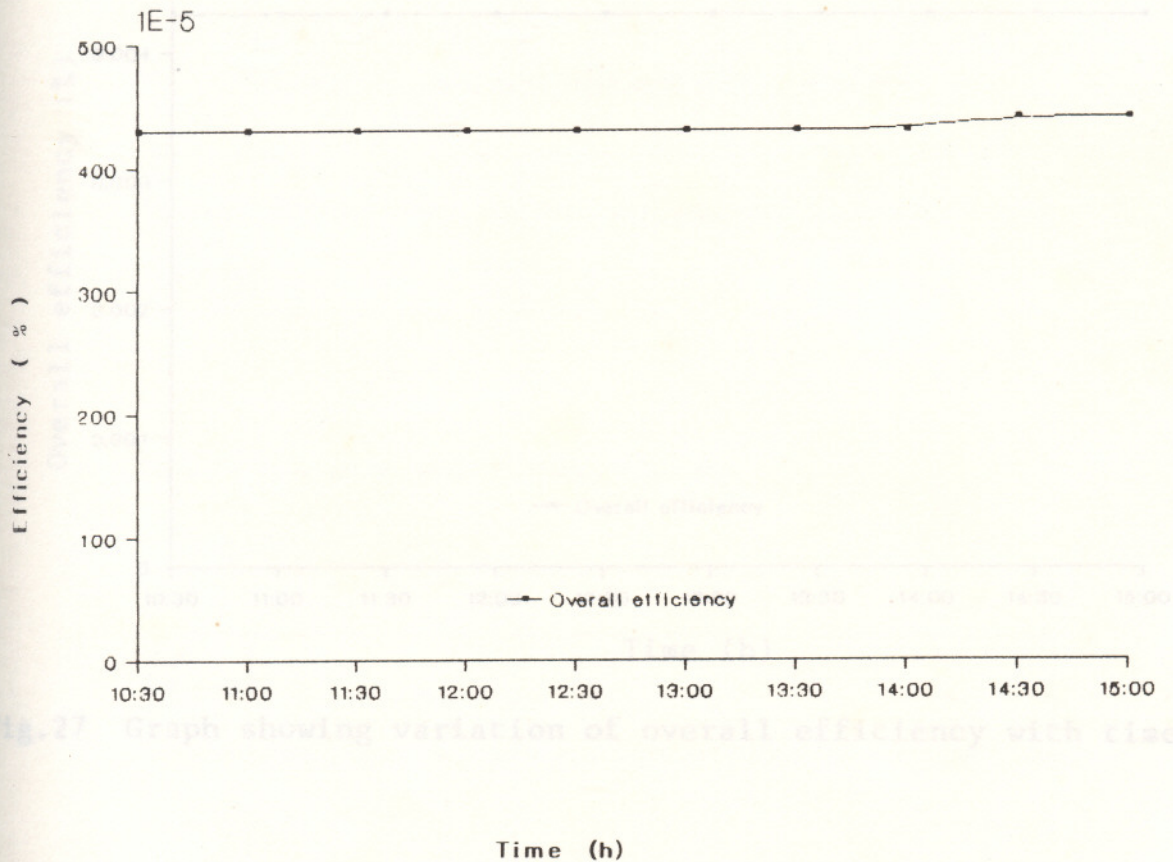


Fig.27 Graph showing variation of overall efficiency with time

Fig.26 Graph showing variation of overall efficiency with time



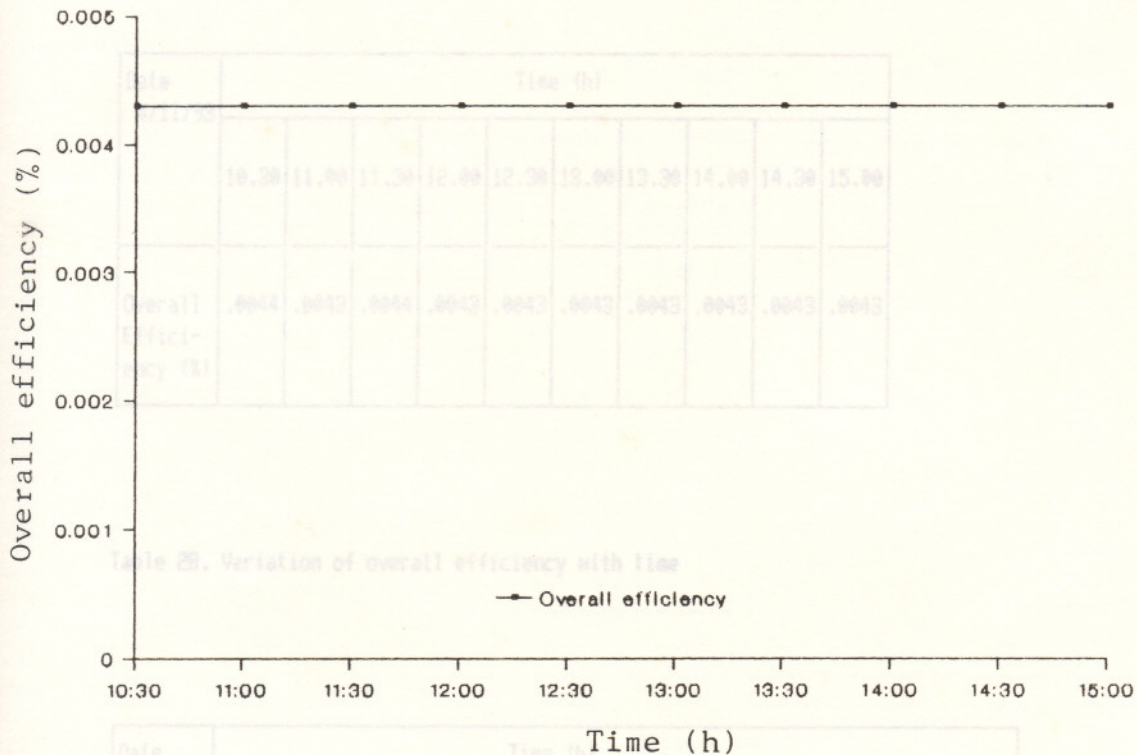


Fig.27 Graph showing variation of overall efficiency with time

Table 27. Variation of overall efficiency with time

Date 4/11/93	Time (h)									
	10.30	11.00	11.30	12.00	12.30	13.00	13.30	14.00	14.30	15.00
Overall Efficiency (%)	.0044	.0043	.0044	.0043	.0043	.0043	.0043	.0043	.0043	.0043

Table 28. Variation of overall efficiency with time

Date 5/11/93	Time (h)											
	12.00	12.30	13.00	13.30	14.00	14.30	15.00	15.30	16.00	16.30	17.00	17.30
Overall Efficiency (%)	.0043	.0043	.0043	.0043	.0043	.0043	.0043	.0043	.0043	.0043	.0044	.0044



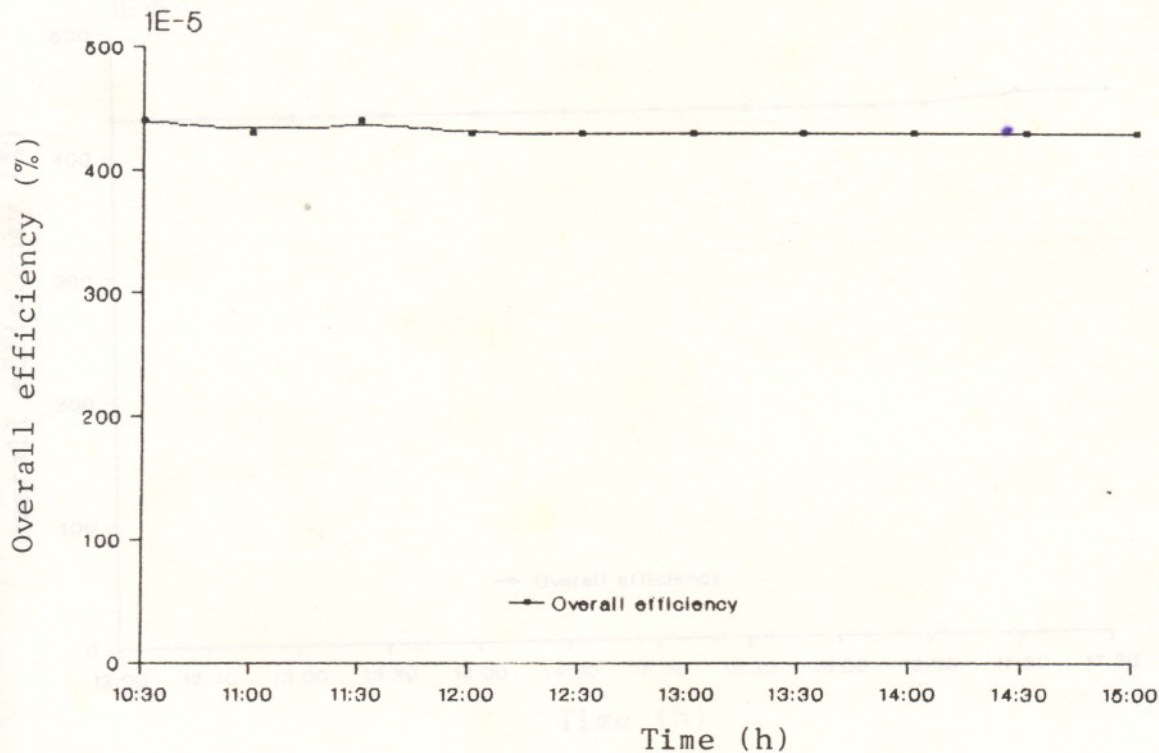


Fig.28 Graph showing variation of overall efficiency with time

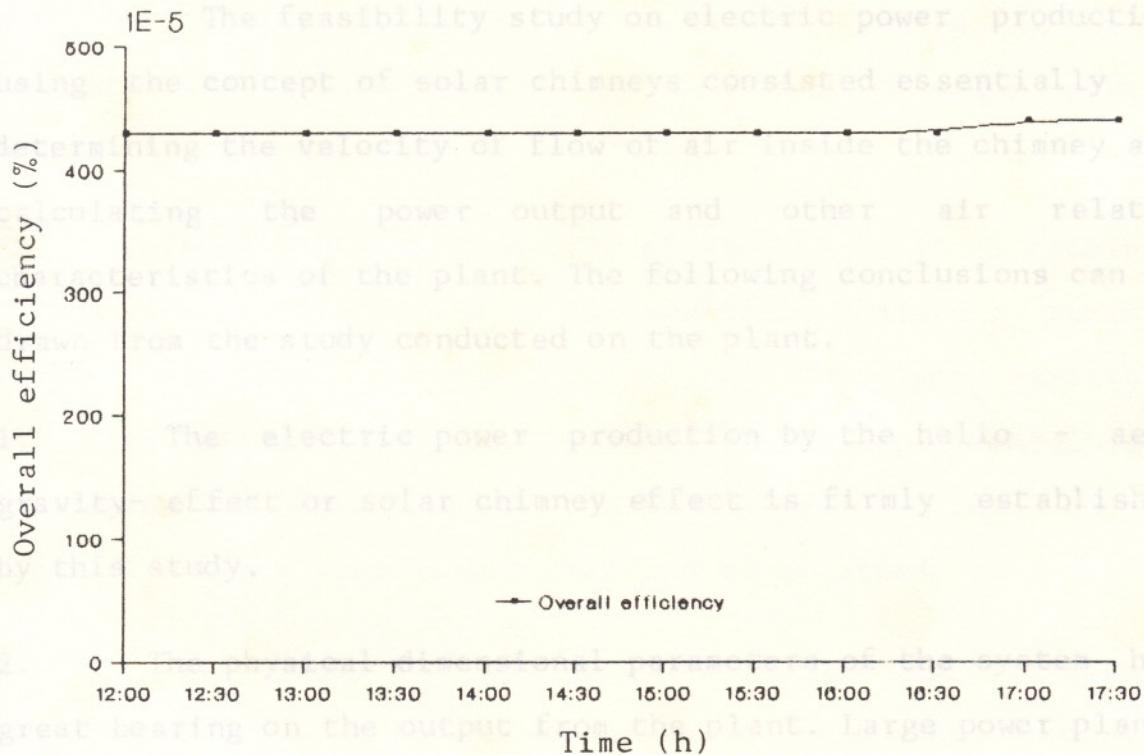


Fig.29 Graph showing variation of overall efficiency with time



## CONCLUSION

The feasibility study on electric power production using the concept of solar chimneys consisted essentially in determining the velocity of flow of air inside the chimney and calculating the power output and other air related characteristics of the plant. The following conclusions can be drawn from the study conducted on the plant.

1. The electric power production by the helio - aero gravity- effect or solar chimney effect is firmly established by this study.

2. The physical dimensional parameters of the system has great bearing on the output from the plant. Large power plants spanning huge areas of land are essential to produce reasonable power output that could be fed to the local power supply grid. The chimney height is the largest single factor which can improve the efficiency and power output from the plant.

3. The height of canopy gap at the periphery of the collector area has to be optimized to reduce the effect of side winds, which otherwise will affect air flow inside the plant.

4. The ground acts as a storage medium storing part of heat energy from the radiations falling on the land surface during the day time. During shady hours and also at night, this heat will be released to warm the surrounding air which in turn can rotate the turbine producing electric power, though at a reduced rate.

5. Temperature differential of about 9 to 15 °C attained during the testing period is sufficient to operate a turbine inside the chimney. The power output from the plant maximises at large values of surface temperature. For experimental set up, selective black coatings can be applied to increase the range of surface temperature that can be attained.

6. The velocity of air obtained at the chimney entrance of about 2.5 m/s is sufficient to start the operation of the turbine under load. The feasibility of the concept of electric power production by the helio-aero-gravity effect or solar chimney effect is proved beyond doubt as it is already a well established and proven technology to run an air turbine at 2.5 m/s with generator connected to it at efficiency levels of about 50 %.

7. This technology is economically feasible only in areas where large tracks of land which cannot be put to any other use is available.



8. The construction of solar chimney power plant envisages technology that is easily available in developing countries like India.

## SUMMARY

Tapping energy from renewable sources is of great interest to energy researchers, technologists, and policy makers due to the the fast depletion of fossil fuels and sharp increase in the global energy demand. Several attempts have been made to exploit solar energy- an inexhaustible non polluting and primary source of energy- for large scale electricity generation. But large scale production of solar electricity and its viable utilisation from an economic point of view have not yet succeeded.

In this context the novel approach of utilising the helio- aero and chimney effects for solar electric energy conversion has significant importance. It consisted of blackened earth surface covered with transparent canopy, a centrally situated chimney and a wind turbine fixed inside the chimney and combining three well known principles viz:- green house effect, chimney effect and wind turbine. This test conducted in K.C.A.E.T., Tavanur, to study the feasibility of the concept of solar chimney had the following objectives:

(i) to verify, establish and demonstrate the operationalisation of the concept



(ii) to generate data correlating the physical parameters of the system with the power produced and

(iii) to determine the overall efficiency of the solar chimney power plant in terms of energy conversion.

A 6m x 6m area was selected, cement coating and black paint were applied to increase the absorptivity to solar radiations. A transparent plastic sheet was used as the canopy above the collector and a PVC pipe of 25cm diameter formed the chimney. To reduce the effects of side winds, the peripheral height of the canopy was kept at 10 cm from the ground.

Tests were conducted in the plant to measure the velocity of air entering the chimney, surface temperature, temperature of air at the inlet to the chimney and the ambient air temperature. These were used to determine the power output from the plant, the overall efficiency of the plant and other plant and air related characteristics.

Test results proved beyond doubt the feasibility of the concept of electric power production using solar chimneys, even though a dynamo of frictionless type could not be obtained for fixing inside the chimney. A maximum velocity of air of 2.47 m/s was obtained at the inlet to the chimney. The temperature of the black collector surface attained a

maximum of 66°C. The temperature differential obtained inside the plant along with the sink effect produced by the chimney was sufficient to generate enough velocity of air in the chimney that the study could be concluded proving the feasibility of the concept of solar chimneys. However the overall efficiency of the experimental plant was only 0.004%.



Garg, H.P. (1982). REFERENCES

Anonymous, (1979). Energy - The Next Twenty Years, sponsored by Ford Foundation, Ballinger Publishing Company : 467.

Anonymous, (1992). 100 MW Solar Power Plant. Global Techno Scan. R.S.Borar : 8 - 9.

Anonymous, (1993). Harvesting Solar Energy from Ponds. CAPART Press Clippings 9 (4) : 61 - 64.

Anonymous, (1993). Asia's Largest Solar Plant. CAPART Press Clippings 9 (4) : 60.

Anonymous, (1993). Congress: Concluding Remarks, WREN (1992). Renewable Energy 3 (2/3): 93-94.

Bansal, N.k., Kleeman Manfred and Meliss Michael, (1990). Renewable Energy Sources and Conversion Technology, Tata Mc-GrawHill Publishing Company Ltd.

Bronicki, Y. & Doron, B. (1990). Small and very small self contained power plants for isolated communities. Solar & Wind Technology 7(1): 79-82.



Garg, H.P. (1982). Treatise on Solar Energy Vol I, Fundamentals of Solar Energy, John Wiley and sons, 39-42.

Ghiorgis-Wolde, W. (1990) An appraisal of the performance of a 10.5 KW SAPVS at a village in Ethiopia. Solar & Wind Technology 7(6):725-734.

Horne, W.E. (1985). Solar thermal photovoltaic electric power generator. Alternative Energy Sources VII, Solar Energy 3. Hemisphere Publishing Corporation. 1021 - 1025.

Kulunk, H. (1985). A prototype solar convection chimney operated under Izmit conditions. Proc. 7<sup>th</sup> MICAES 1985, ed. T.N. Veziroglu et al. : 162 - 166.

Kut David and Hare Gerard, (1983). Applied Solar Energy. Butterworths.

Lodhi, M.A.K., Sulaiman Yusof, M. and Ibrahim Shaharin (1989). A Solar Bowl electric power plant for normal solar flux :247 - 254.

Lodhi, M.A.K. and Sulaiman Yusof, M. (1991). Helio-Aero-Gravity electric power production at low cost. Renewable Energy 2 (2): 183-189.



Magal, B.S. (1990). Solar Power Engineering. Tata Mc-Graw Hill Publishing Company Ltd.

Marcotte Boy, J.L., Dancette, M., Bliaux, J., Bacconnet, E. and Malherbe, J. (1985). Construction of a 100 kW Solar-Thermal Electric Experimental Plant. Journal of Solar Energy Engineering 107 : 196- 201.

Radosevich, L.G. and Skinrood, A.C. (1989). The Power Production Operation of Solar One, the 10 MWe Solar Thermal Central Receiver Pilot Plant. Journal of Solar Energy Engineering III.:144-151

Rai, G.D. (1991). Solar Energy Utilisation. Khanna Publishers.

Scesa, S. (1985 ). Cooling Tower Retrofit for Solar Power Generation. Alternative Energy Sources VII Solar Energy 2. Hemisphere Publishing Corporation: 459-468.

Schlaich, Bergerman and Partner. (1992). The Or System: Stretched Membrane Concentrators with Stirling Engines. Brochure.



Schlaich Jorg, Schiel Wolfgang, Friedrich Karl. (1992). Solar Chimneys. Encyclopaedia of Physical Science and Technology. 15: 335-343.

Schaefer,H. and Hagedorn,G. (1992). Hidden Energy and Correlated Environmental Characteristics of PV Power Generation. Renewable Energy - An International Journal. 2(2): 159 - 166.

Shousha,A.H.M. (1989). Performance Characteristics of Thin Film MIS Solar Cells. Solar & Wind Technology 6(6): 705-712.

Sukhatme,S.P. (1984). Solar Energy - Principles of Thermal Collection and Storage Tata McGraw Hill Publishing Company Ltd.

Sukhatme,S.P. (1992). Large Scale Electrical Power Generation Through the Solar Thermal Route. Journal of Solar Energy Society of India 2(1): 35-40.

Torralbo Munoz,A., Gonzalvez Hernandez,C., Roses Ortiz,C., Lacal Avellaner,J. and Sanchez,F. (1984). A Spanish Power Tower Solar System: Project CESA - 1. Journal of Solar Energy Engineering 106 : 78-82.

Zvirin,Y. and Zamkow,S. (1993). Solar Energy in Israel - Utilisation and Research. Journal of Energy, Heat and Mass Transfer 15: 145-164.



## APPENDIX - I

Make : OTA KEIKI, Japan.

Instrumentation. Number : 232412

Number of blades : 8

### a. Specification of the solar intensity meter

Range : 0 to 1 00 000 m

Name : Suryamapi

Model Number : SM 201

Range of Electronic digital :

0 - 120 mW/cm<sup>2</sup>

Supplied by : Central Electronics Ltd.

Name : ACD electronic digital

### b. Specification of digital thermometer:

Range : upto 30 s/s

### Technical specification.

Power Supply : 230 V AC 50 Hz supply or 6

Sensor type : Thermocouple K (NiCr-NiAl)

Resolution : 1 °C

Accuracy : +\_1 %

Measurement

range : -50 °C to 800 °C

### General Specification

Display : LCD, 0.5"

Power Supply : DC 9 V battery.

Dimension : 0.8 x 2.8 x 4.2 inch.

Weight : 120 g including battery.

Impedence : 10 M Ohms.

### c. Specification of Vane Anemometer.

Make : OTA KEIKI, Japan.

Serial Number : 232412

Number of blades : 8

Range : 0 to 1 00 000 m

Possible measuring  
wind speed : 1 to 15 m/s

### d. Specification of Electronic Anemometer digital.

Name : ACD electronic digital display  
anemometer.

Range : upto 30 m/s

Power Supply : 230 V AC 50 Hz supply or 6 x 1.5 V type  
UM - 2 V batteries.

Supplied by : Electronics Instruments Co., Bombay.



## APPENDIX - II

Specification of the materials used for the prototype Solar chimney plant at Tavanur.

Sl.No.	Item	Specification
1.	Canopy	Material - Clear plastic. Size - 7 m x 7m square.
2.	Solar Chimney	Material - PVC pipe. Gauge - 2.5 Kg/cm <sup>2</sup> . Length - 6 m. Diameter (inside) - 25 cm.
3.	Black Paint	Quantity - 5 l
4.	Cement	Quantity - 2.5 bags (125 Kg).
5.	Posts at corner points & midpoints of Collector side	Material - angle iron. Number - 8. Size - 1.25" and 0.25"
6.	Stay Wire	Material - GI wire Gauge - 14 Length - 36 m
7.	Canopy Support	Material - GI wire. Gauge - 14 Length - 110 m.

8. Bolts

Material - mild steel

Number - 8

Size - 5/8 "

length - 6".

9. Hook

Material - mild steel

Number - 16.

Size - 1" inside diameter.

10. Chimney Support

Material - MS rods

a) Size - 18 mm diameter.

Length - 120 cm.

Number - 3.

b) Size - 5 mm diameter.

Length - 90 cm

Number - 3.

c) Material - MS flat

Number - 2

Width - 1", 1.5"



## APPENDIX III

## Test results of 07-10-93

Sl. No.	Time (h)	I <sup>2</sup> W/m	T <sub>a</sub> °C	T <sub>m</sub> °C	T <sub>s</sub> °C	v (m/s)	$\rho_a$ <sup>3</sup> (kg/m <sup>3</sup> )	$\rho_m$ <sup>3</sup> (kg/m <sup>3</sup> )	C <sub>p</sub> J/Kg°K	$\dot{m}$ Kg/s	$\Delta p$ (Pa)	P <sub>a</sub> (W)	P <sub>r</sub> (W)	$\eta_w$ (%)	$\eta_o$ (%)
1	12.00	500	35	46	54	2.32	1.146	1.107	1005	0.1261	2.325	0.776	0.170	0.0190	0.0043
2	12.30	650	36	47	56	2.47	1.143	1.104	1005	0.1338	2.325	1.005	0.204	0.0191	0.0043
3	13.00	500	33	39	50	1.89	1.154	1.132	1005	0.1050	1.307	0.781	0.094	0.0192	0.0043
4	13.30	400	32	38	48	2.33	1.158	1.135	1005	0.1299	1.307	0.627	0.176	0.0191	0.0044

I - Insolation

T<sub>a</sub> - Ambient temperatureT<sub>m</sub> - Maximum temperatureT<sub>s</sub> - Surface temperature

v - Measured velocity

 $\rho_a$  - Density of air at ambient temperature $\rho_m$  - Density of air at maximum temperatureC<sub>p</sub> - Specific heat of air $\dot{m}$  - Mass flow rate $\Delta P$  - Pressure difference between top and bottom of chimneyP<sub>a</sub> - Expected average output of SCPPP<sub>r</sub> - Rotor power $\eta_w$  - Efficiency with which thermal power is converted to wind power $\eta_o$  - Overall efficiency



## APPENDIX IV

Test results of 14-10-93

Sl. No.	Time (h)	I <sup>2</sup> W/m	T <sub>a</sub> °C	T <sub>m</sub> °C	T <sub>s</sub> °C	v (m/s)	ρ <sub>a</sub> <sup>3</sup> (kg/m <sup>3</sup> )	ρ <sub>m</sub> <sup>3</sup> (kg/m <sup>3</sup> )	C <sub>p</sub> J/Kg*K	ṁ Kg/s	ΔP (Pa)	P <sub>a</sub> (W)	P <sub>r</sub> (W)	η <sub>w</sub> (%)	η <sub>o</sub> (%)
1	13.30	960	33	47	60	2.33	1.1539	1.1035	1005	0.1262	2.967	1.499	0.1713	0.0191	0.0043
2	13.45	900	33	45	53	2.06	1.1539	1.1105	1005	0.1123	2.555	1.406	0.1191	0.0191	0.0043
3	14.00	960	35	48	62	2.17	1.1465	1.1000	1005	0.1172	2.737	1.490	0.1379	0.0190	0.0043
4	14.15	1000	37	50	66	2.45	1.1391	1.0930	1005	0.1314	2.713	1.541	0.1973	0.0190	0.0043
5	14.30	880	36	48	57	1.80	1.1430	1.1000	1005	0.0972	2.531	1.361	0.0787	0.0190	0.0043

I - Insolation

T<sub>a</sub> - Ambient temperatureT<sub>m</sub> - Maximum temperatureT<sub>s</sub> - Surface temperature

v - Measured velocity

ρ<sub>a</sub> - Density of air at ambient temperatureρ<sub>m</sub> - Density of air at maximum temperatureC<sub>p</sub> - Specific heat of air

ṁ - Mass flow rate

ΔP - Pressure difference between top and bottom of chimney

P<sub>a</sub> - Expected average output of SCPP<sub>r</sub> - Rotor powerη<sub>w</sub> - Efficiency with which thermal power is converted to wind powerη<sub>o</sub> - Overall efficiency



## Test results of 16-10-93

Sl. No.	Time (h)	I <sup>2</sup> W/m	T <sub>a</sub> °C	T <sub>m</sub> °C	T <sub>s</sub> °C	v (m/s)	$\rho_a$ <sup>3</sup> (kg/m <sup>3</sup> )	$\rho_m$ <sup>3</sup> (kg/m <sup>3</sup> )	C <sub>p</sub> J/Kg*K	$\dot{m}$ Kg/s	$\Delta P$ (Pa)	P <sub>a</sub> (W)	P <sub>r</sub> (W)	$\eta_w$ (%)	$\eta_o$ (%)
1	10.30	570	33	40	45	1.66	1.154	1.128	1005	0.0919	1.530	0.890	0.063	0.019	0.0043
2	11.00	700	34	42	49	1.70	1.150	1.121	1005	0.0935	1.707	1.0897	0.068	0.019	0.0043
3	11.30	860	35	47	56	1.80	1.147	1.104	1005	0.0975	2.531	1.3340	0.079	0.019	0.0043
4	12.00	1010	36	49	58	2.39	1.143	1.097	1005	0.1287	2.707	1.562	0.184	0.019	0.0043
5	12.30	720	35	48	56	1.72	1.147	1.100	1005	0.0929	2.766	1.117	0.069	0.019	0.0043
6	13.00	630	34	47	56	1.70	1.150	1.104	1005	0.0921	2.707	0.981	0.067	0.019	0.0043
7	13.30	460	33	45	55	2.03	1.154	1.111	1005	0.1107	2.531	0.718	0.114	0.019	0.0043
8	14.00	440	33	44	55	1.62	1.154	1.114	1005	0.0886	2.354	0.687	0.058	0.021	0.0043
9	14.30	400	32	41	54	1.58	1.158	1.123	1005	0.0871	2.060	0.627	0.054	0.020	0.0044
10	15.00	300	32	41	53	1.50	1.158	1.123	1005	0.0827	2.060	0.470	0.046	0.020	0.0044

I - Insolation

T<sub>a</sub> - Ambient temperatureT<sub>m</sub> - Maximum temperatureT<sub>s</sub> - Surface temperature

v - Measured velocity

 $\rho_a$  - Density of air at ambient temperature $\rho_m$  - Density of air at maximum temperatureC<sub>p</sub> - Specific heat of air $\dot{m}$  - Mass flow rate $\Delta P$  - Pressure difference between top and bottom of chimneyP<sub>a</sub> - Expected average output of SSCPP<sub>r</sub> - Rotor power $\eta_w$  - Efficiency with which thermal power is converted to wind power $\eta_o$  - Overall efficiency



## APPENDIX VI

Test results of 31-10-93

Sl. No.	Time (h)	I <sup>2</sup> W/m	T <sub>a</sub> °C	T <sub>m</sub> °C	T <sub>s</sub> °C	v (m/s)	$\rho_a$ <sup>3</sup> (kg/m <sup>3</sup> )	$\rho_m$ <sup>3</sup> (kg/m <sup>3</sup> )	C <sub>p</sub> J/Kg°K	$\dot{m}$ Kg/s	$\Delta p$ (Pa)	P <sub>a</sub> (W)	P <sub>r</sub> (W)	$\eta_w$ (%)	$\eta_o$ (%)
1	10.30	940	33	43	49	1.96	1.154	1.118	1005	0.108	2.119	1.468	0.103	0.0190	0.0043
2	11.00	1010	33	45	52	2.02	1.154	1.111	1005	0.110	2.531	1.577	0.112	0.0190	0.0043
3	11.30	1020	33	46	52	2.1	1.154	1.107	1005	0.114	2.766	1.593	0.126	0.0191	0.0043
4	12.00	1080	35	48	61	2.34	1.147	1.100	1005	0.126	2.766	1.676	0.173	0.0192	0.0043
5	12.30	1060	34	46	57	2.31	1.150	1.107	1005	0.126	2.531	1.650	0.167	0.0190	0.0043
6	13.00	960	33	46	56	2.24	1.154	1.107	1005	0.122	2.766	1.499	0.153	0.0191	0.0043
7	13.30	900	33	45	55	2.23	1.154	1.111	1005	0.122	2.531	1.406	0.151	0.0190	0.0043
8	14.00	900	33	47	56	2.28	1.154	1.104	1005	0.124	2.943	1.406	0.161	0.0190	0.0043
9	14.30	860	33	45	55	2.20	1.154	1.111	1005	0.120	2.531	1.343	0.145	0.0190	0.0043
10	15.00	800	33	44	55	2.15	1.154	1.114	1005	0.118	2.354	1.249	0.136	0.0191	0.0043

I - Insolation

T<sub>a</sub> - Ambient temperatureT<sub>m</sub> - Maximum temperatureT<sub>s</sub> - Surface temperature

v - Measured velocity

 $\rho_a$  - Density of air at ambient temperature $\rho_m$  - Density of air at maximum temperatureC<sub>p</sub> - Specific heat of air $\dot{m}$  - Mass flow rate $\Delta p$  - Pressure difference between top and bottom of chimneyP<sub>a</sub> - Expected average output of SCPPP<sub>r</sub> - Rotor power $\eta_w$  - Efficiency with which thermal power is converted to wind power $\eta_o$  - Overall efficiency



## Test results of 04-11-93

Sl. No.	Time (h)	I W/m <sup>2</sup>	Ta °C	Tm °C	Ts °C	v (m/s)	$\rho_a$ (kg/m <sup>3</sup> )	$\rho_m$ (kg/m <sup>3</sup> )	Cp J/kg*°K	$\dot{m}$ Kg/s	$\Delta p$ (Pa)	Pa (W)	Pr (W)	$\eta_w$ (%)	$\eta_o$ (%)
1	10.30	680	32	38	48	1.44	1.158	1.135	1005	0.0802	1.354	1.065	0.0416	0.0198	0.0044
2	11.00	200	32	34	44	1.30	1.158	1.150	1005	0.0733	0.479	0.313	0.0310	0.0207	0.0043
3	11.30	600	32	36	47	1.43	1.158	1.143	1005	0.0802	0.883	0.940	0.0410	0.0192	0.0044
4	12.00	900	32	39	51	2.01	1.154	1.132	1005	0.1117	1.295	1.406	0.1128	0.0190	0.0043
5	12.30	900	33	44	55	2.12	1.150	1.114	1005	0.1159	2.119	1.401	0.1303	0.0190	0.0043
6	13.00	800	34	45	55	2.10	1.150	1.111	1005	0.1145	2.296	1.245	0.1263	0.0205	0.0043
7	13.30	800	34	47	56	2.05	1.150	1.104	1005	0.1110	2.707	1.245	0.1167	0.0190	0.0043
8	14.00	760	34	47	56	2.27	1.150	1.104	1005	0.1230	2.707	1.183	0.1585	0.0190	0.0043
9	14.30	400	33	43	55	1.88	1.154	1.118	1005	0.1032	2.119	0.625	0.0912	0.0190	0.0043
10	15.00	200	33	41	54	2.01	1.154	1.123	1005	0.1108	1.825	0.312	0.1119	0.0202	0.0043

I - Insolation

Ta - Ambient temperature

Tm - Maximum temperature

Ts - Surface temperature

v - Measured velocity

 $\rho_a$  - Density of air at ambient temperature $\rho_m$  - Density of air at maximum temperature

Cp - Specific heat of air

 $\dot{m}$  - Mass flow rate $\Delta p$  - Pressure difference between top and bottom of chimney

Pa - Expected average output of SSCP

Pr - Rotor power

 $\eta_w$  - Efficiency with which thermal power is converted to wind power $\eta_o$  - Overall efficiency



APPENDIX VIII

Test results of 05-11-93

Sl. No.	Time (h)	I W/m <sup>2</sup>	T <sub>a</sub> °C	T <sub>m</sub> °C	T <sub>s</sub> °C	v (m/s)	ρ <sub>a</sub> (kg/m <sup>3</sup> )	ρ <sub>m</sub> (kg/m <sup>3</sup> )	C <sub>p</sub> J/Kg*°K	ṁ Kg/s	Δp (Pa)	P <sub>a</sub> (W)	P <sub>r</sub> (W)	η <sub>w</sub> (%)	η <sub>o</sub> (%)
1	12.00	940	34	43	57	2.21	1.150	1.118	1005	0.121	1.883	1.463	0.1481	0.0186	0.0043
2	12.30	940	34	44	61	2.06	1.150	1.114	1005	0.113	2.119	1.463	0.1195	0.0188	0.0043
3	13.00	900	34	43	58	2.06	1.150	1.118	1005	0.113	1.883	1.401	0.1199	0.0186	0.0043
4	13.30	820	34	42	54	2.22	1.150	1.121	1005	0.122	1.707	1.276	0.1505	0.0190	0.0043
5	14.00	800	34	43	56	2.23	1.150	1.118	1005	0.122	1.883	1.245	0.1521	0.0186	0.0043
6	14.30	600	33	45	56	2.12	1.154	1.111	1005	0.116	2.531	0.937	0.1299	0.0188	0.0043
7	15.00	530	33	43	55	1.91	1.154	1.118	1005	0.105	2.119	0.828	0.0956	0.0189	0.0043
8	15.30	420	33	42	53	2.10	1.154	1.121	1005	0.116	1.942	0.656	0.1274	0.0192	0.0043
9	16.00	600	33	43	55	1.98	1.154	1.118	1005	0.109	2.119	0.937	0.1065	0.0189	0.0043
10	16.30	540	32	41	51	1.74	1.158	1.125	1005	0.096	1.942	0.843	0.0727	0.0192	0.0043
11	17.00	400	32	39	47	1.80	1.158	1.132	1005	0.100	1.530	0.627	0.0810	0.0195	0.0044
12	17.30	100	30	31	42	1.69	1.165	1.162	1005	0.096	0.177	0.158	0.0688	0.0158	0.0044

I - Insolation

T<sub>a</sub> - Ambient temperature

T<sub>m</sub> - Maximum temperature

T<sub>s</sub> - Surface temperature

v - Measured velocity

ρ<sub>a</sub> - Density of air at ambient temperature

ρ<sub>m</sub> - Density of air at maximum temperature

C<sub>p</sub> - Specific heat of air

ṁ - Mass flow rate

ΔP - Pressure difference between top and bottom of chimney

P<sub>a</sub> - Expected average output of SCPP

P<sub>r</sub> - Rotor power

η<sub>w</sub> - Efficiency with which thermal power is converted to wind power

η<sub>o</sub> - Overall efficiency



# FEASIBILITY STUDY ON ELECTRIC POWER PRODUCTION BY THE HELIO - AERO - GRAVITY EFFECT

By

GANESH. B.  
JEEJA C. K.

## ABSTRACT OF THE PROJECT REPORT

Submitted in partial fulfilment of the  
requirement for the degree of

### Bachelor of Technology in Agricultural Engineering

Faculty of Agricultural Engineering & Technology  
Kerala Agricultural University

Department of Farm Power Machinery and Energy  
Kelappaji College of Agricultural Engineering and Technology

Tavanur - 679 573

Malappuram

1993

## ABSTRACT

The energy crisis that has gripped the world after the 1970's has led to the development of various technologies, utilising renewable sources for power production. An economically viable technology for solar electric energy conversion is yet to be developed. In this context, the novel concept of solar chimney power plant, consisting of blackened earth surface covered with transparent canopy, a centrally situated chimney and a wind turbine fixed inside the chimney has significant relevance. A study was conducted in K.C.A.E.T., Tavanur, to test the feasibility of this concept. A microscale prototype solar chimney plant was set up as part of this study. The tests conducted in the plant proved beyond doubt the feasibility of the concept of solar chimneys. Maximum air velocity of 2.47 m/s was attained at the inlet to the chimney. The temperature of the black collector surface reached a maximum of 66°C when the insolation was quite high. The results pointed out the fact that large solar power plants can produce electric power which could be supplied to the power supply grid of the region.